THE SAFFMAN–TAYLOR PROBLEM FOR AN EXTREMELY SHEAR-THINNING FLUID

by G. RICHARDSON † *and* J. R. KING

(*Section of Theoretical Mechanics, University of Nottingham, Nottingham* NG7 2RD)

[Received 2 August 2006. Revise 16 January 2007]

Summary

We consider a steady flow driven by pushing a finger of gas into a highly shear-thinning power-law fluid, with exponent n, in a Hele-Shaw channel. We formulate the problem in terms of the streamfunction ψ, which satisfies the p-Laplacian equation $\nabla \cdot (|\nabla \psi|^{p-2} \nabla \psi) = 0$ (with $p = (n+1)/n$), and investigate travelling wave solutions in the large-n (extreme shear-thinning) limit. We take a Legendre transform of the free-boundary problem for ψ, which reduces it to a linear problem on a fixed domain. The solution to this problem is found by using matched asymptotic expansions and the resulting shape of the finger deduced (being, to leading order, a semi-infinite strip). The nonlinear problem for the streamfunction is also treated using matched asymptotic expansion in the physical plane. The finger-width selection problem is briefly discussed in terms of our results.

1. Introduction

The Saffman–Taylor problem has been the subject of a great deal of interest for nearly fifty years. It was initially posed in order to describe experiments by Saffman and Taylor (**1**). These involved pushing a finger of air into a Hele-Shaw channel, filled with a Newtonian liquid, under the action of a pressure difference. It was observed that the ratio λ of the selected finger width to that of the channel is one-half (except when the injection is very slow). In addition, Saffman and Taylor (**1**) derived a family of zero surface tension solutions, parametrized by λ, describing the finger shape. Finger-width selection remained unexplained until a numerical calculation of finger shape, in the presence of surface tension, was performed by McLean and Saffman (**2**). Subsequently asymptotic methods have been used to derive the celebrated result $\lambda = 1/2$ in the limit of low surface tension (or high finger velocity) (**3** to **5**), as well as in limiting cases of other regularizations such as kinetic undercooling (**6**) (see also (**7**) for a review of the subject). We stress, however, that there are other circumstances in which the selected finger does not have $\lambda = 1/2$ (see (**8**), in particular), including the near-Newtonian limit of power-law fluids (**9**, **10**).

Hele-Shaw flows of power-law fluids (with general exponent n; see (4) below) have been investigated by Aronsson and Janfalk (**11**), who obtain similarity solutions describing (i) flow about a corner (ii) doublet flows and (iii) spiral flows. The Hele-Shaw free-boundary problem, describing the motion of an interface between air and fluid, was considered by King (**12**), who investigated a local problem describing the flow in the vicinity of a corner in the free boundary. In particular, (**12**) shows that under injection the corner persists for finite time if its angle is less than some critical angle, whereas if it exceeds this angle the corner immediately smooths. Under suction the corner

†⟨Giles.Richardson@nottingham.ac.uk⟩

doi:10.1093/qjmam/hbm003

persists, if its angle is subcritical, until the solution ceases to exist. Saffman–Taylor type problems for power-law fluids have been investigated by Alexandrou and Entov (**13**), who consider the zero surface tension case, and Ben Amar and Corvera Poiré (**9**, **10**) who investigate the near-Newtonian limit ($|n-1| \ll 1$) and postulate that for shear-thinning fluids the selected finger width λ decreases towards zero as the surface tension σ tends to zero.

It is the aim of this work to find asymptotic solutions to the Saffman–Taylor problem in which a symmetric finger of air is pushed into a Hele-Shaw channel, filled with a strongly shear-thinning power-law fluid. Such extreme shear-thinning fluid flows give rise to highly-nonlinear elliptic partial differential equations (PDEs) for both the stream function ψ and the pressure p, corresponding to the limit $n \to \infty$ in

$$\nabla \cdot \left(\frac{\nabla \psi}{|\nabla \psi|^{1-1/n}} \right) = 0, \quad \nabla \cdot (|\nabla p|^{n-1} \nabla p) = 0, \tag{1}$$

respectively. In the context of such flows we note that considerable progress has been made, in this limit, on injection problems (whereby fluid is injected into a Hele-Shaw cell at one or more points) by Aronsson and co-workers; see, in particular, (**14**) which describes how, in the absence of surface tension, the free boundary of the fluid follows the level sets of an interior distance function centred on the injection points. At its most basic level this approach consists in noting that the 'naive' limit of the streamfunction problem (1) is the degenerate one

$$\nabla \cdot \left(\frac{\nabla \psi}{|\nabla \psi|} \right) = 0. \tag{2}$$

This limit problem for ψ is parabolic and the associated streamlines (lines on which ψ is constant) are, necessarily in the two-dimensional case treated here, straight lines: equation (2) simply states that the level sets of ψ have zero mean curvature. It is informative to compare this with the corresponding limit problem for the pressure equation (1a), namely the eikonal equation

$$|\nabla p| = 1, \tag{3}$$

whose rays correspond to the level sets of ψ. (The correspondence between these two equations has previously been noted in (**15**, Appendix D). The degeneracy of the large n limit is reflected by the fact that, as for the limit problem for the streamfunction (2), this (eikonal) equation is non-elliptic. We remark that (2) thus belongs to the (exceptional) class of second-order parabolic equations that can be mapped to first-order hyperbolic ones (whose characteristic projections coincide with the repeated characteristics of the parabolic problem). In the context of the injection problem, the zero-pressure condition on the free boundary, which can also be expressed as the normal derivative condition $\partial \psi / \partial N|_{\partial \Omega} = 0$, implies that the streamlines meet the free boundary perpendicularly. Thus an evolving free boundary consists of arcs of circles centred on each of the injection points (see Fig. 1a). This of course ignores what happens on sections of the free boundary that do not initially form such circular arcs. However, provided a point on the boundary is further from the injection point than the smallest distance between injection point and boundary, its velocity is exponentially small in n; thus such boundary points move exponentially slowly (see Fig. 1b). This type of argument has been rigorously formulated as a *distance model* by Aronsson (**14**). Piscotti *et al.* (**16**) have favourably compared solutions to this model with their experiments in which polystyrene is injected into an industrial mould. In particular, they find that the model accurately predicts the weld lines, even when the polystyrene formulation has only moderately shear-thinning properties. Other applications of this model in such industrial contexts are described in (**17**). Squeeze

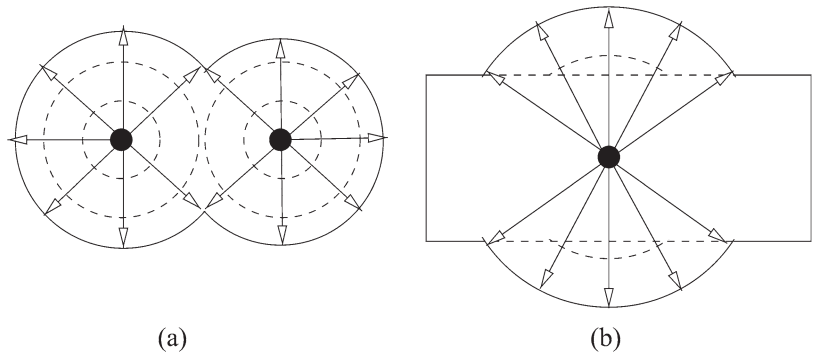

Fig. 1 Injection from (a) two points with no fluid initially present and (b) from a single point into an initially rectangular domain. Here dashed lines show previous positions of the fluid domain, while the solid one shows the present position. Lines with arrows show the asymptotic streamlines

film Hele-Shaw flows of extremely shear-thinning fluids (with applications to compression moulding) have been investigated by Aronsson and Evans (**18**) and Bergwall (**19**). The extreme shear-thinning limit of power-law fluid flows has also been considered, outside the Hele-Shaw context, by Brewster *et al.* (**20**) and Chapman *et al.* (**21**), who observe that even simple flows, such as Jeffrey–Hamel flows in a wedge, exhibit a rich asymptotic structure. The time-dependent version of the large-n limit of (1b) has also been considered in the context of Bean model, which models the motion of superconducting vortices in so-called 'dirty' superconductors; see, for example, (**22**).

Little, however, is known about the corresponding Hele-Shaw suction problem other than that it is ill-posed (see, for example, (**12**)). A number of works consider the Saffman–Taylor problem for power-law fluids in a channel. In (**9**, **10**) a semi-numerical, semi-asymptotic method is used to study the Saffman–Taylor finger selection problem in the limit of $n \to 1$ (that is, for a nearly-Newtonian fluid). For $O(1)$ values of the dimensionless surface tension the finger width is little changed from its Newtonian value, but for small surface tension there is a significant decrease in finger width as n increases above unity. Alexandrou and Entov (**13**) construct symmetric Saffman–Taylor fingers for arbitrary values of the power-law exponent n (and for Bingham fluids) but with zero surface tension (ZST) on the free boundary. In order to do this they apply a linearizing hodograph transformation to the problem, resulting in a linear elliptic PDE on a fixed domain in the hodograph plane that is solved numerically. Although this approach cannot predict finger width, it does predict finger shape and (**13**, Fig. 3) is suggestive of our results below that in the large-n limit this approaches a semi-infinite strip. Experimental studies of viscous fingering (and of finger-width selection) in non-Newtonian fluids have been conducted by Lindner *et al.* (**23**, **24**), with the conclusion that narrow fingers are selected in shear-thinning fluids.

2. Problem formulation

The velocity of the fluid $\boldsymbol{w}$ is given in terms of the pressure p by (working throughout in dimensionless terms)

$$\boldsymbol{w} = -|\nabla p|^{n-1}\nabla p. \tag{4}$$

Assuming incompressibility leads to

$$\nabla \cdot \left(|\nabla p|^{n-1} \nabla p \right) = 0.$$

Alternatively, the problem can be formulated in terms of the stream function ψ defined by

$$\boldsymbol{w} = \frac{\partial \psi}{\partial y} \boldsymbol{e}_x - \frac{\partial \psi}{\partial x} \boldsymbol{e}_y. \tag{5}$$

This leads to following 'Cauchy–Riemann' relations between p and ψ:

$$\frac{\partial p}{\partial x} = -\frac{1}{|\nabla \psi|^{1-1/n}} \frac{\partial \psi}{\partial y}, \quad \frac{\partial p}{\partial y} = \frac{1}{|\nabla \psi|^{1-1/n}} \frac{\partial \psi}{\partial x},$$

and hence to

$$\nabla \cdot \left(\frac{\nabla \psi}{|\nabla \psi|^{1-1/n}} \right) = 0; \tag{6}$$

it is noteworthy that, though they are of different order, equations (2) and (3) can be mapped to each other via

$$\frac{\partial p}{\partial x} = -\frac{1}{|\nabla \psi|} \frac{\partial \psi}{\partial y}, \quad \frac{\partial p}{\partial y} = \frac{1}{|\nabla \psi|} \frac{\partial \psi}{\partial x}.$$

Without loss of generality we consider the finger to move with unit (dimensionless) velocity in the x-direction. In the case of zero surface tension the boundary conditions on the free boundary $\partial \boldsymbol{\Omega}_f$ (with outward normal $\boldsymbol{N}$) are

$$p|_{\partial \Omega_f} = 0, \quad \boldsymbol{N} \cdot \boldsymbol{w}|_{\partial \Omega_f} = \boldsymbol{e}_x \cdot \boldsymbol{N}, \tag{7}$$

the latter equation corresponding to the kinematic condition in this travelling wave case. We can rewrite these in terms of ψ as

$$\left. \frac{\partial \psi}{\partial N} \right|_{\partial \Omega_f} = 0, \quad \left. \frac{\partial \psi}{\partial s} \right|_{\partial \Omega_f} = \boldsymbol{e}_x \cdot \boldsymbol{N}, \tag{8}$$

where s is arc length along the boundary. In addition, boundary conditions on the edges of the Hele-Shaw cell (namely the impermeable channel walls $y = -1$ and $y = 1$) must be imposed. Assuming a finger of width 2λ, the flux of fluid through a cross-section of the cell is 2λ and we may choose the origin of ψ such that

$$\psi|_{y=1} = \lambda, \quad \psi|_{y=-1} = -\lambda. \tag{9}$$

Imposing symmetry about the centreline $x = 0$, so that $\psi|_{y=0} = 0$, integrating $(8)_2$ and collating the equations and boundary conditions for ψ gives the following closed problem, if λ is specified, which determines ψ up to an arbitrary translation in x:

$$\nabla \cdot \left(\frac{\nabla \psi}{|\nabla \psi|^{1-1/n}} \right) = 0, \tag{10}$$

$$\left. \frac{\partial \psi}{\partial N} \right|_{\partial \Omega_f} = 0, \quad \psi|_{\partial \Omega_f} = y, \tag{11}$$

$$\psi \sim \lambda y \quad \text{as } x \to \infty, \tag{12}$$

$$\psi|_{y=1} = \lambda, \quad \psi|_{y=0} = 0, \quad \psi \to \lambda \quad \text{as } x \to -\infty. \tag{13}$$

The main aim of this work to find an asymptotic solution to this problem in the highly-nonlinear (strongly shear-thinning) limit $n \to \infty$.

3. The Legendre transform

In order to analyse (10) to (13) it is helpful first to reformulate them using a Legendre transform. This has the benefit that the transformed variable satisfies a linear problem in a fixed domain. In this context we note, first, that Atkinson and Champion (**25**), for example, have used this approach to derive exact solutions to equation (1) (although they term this transformation a 'hodograph transform') and, secondly, that Alexandrou and Entov (**13**) have instead used a hodograph transform (that is, in the notation below, ψ is calculated as a function of a and b); although the latter approach also linearizes the problem, it proves more difficult to invert the solution of the transformed problem to obtain the physical variables. The Legendre transform is accomplished by introducing three new variables

$$a = \psi_x, \quad b = \psi_y, \quad \Psi = x\psi_x + y\psi_y - \psi \tag{14}$$

(henceforth such subscripts denote derivatives). Differentiating Ψ with respect to x and y and using the fact that $a_y = b_x$ gives rise, in the usual way, to the inversion formulae

$$x = \Psi_a, \quad y = \Psi_b, \quad \psi = a\Psi_a + b\Psi_b - \Psi. \tag{15}$$

The following expressions for the second derivatives of ψ can then be derived by using the chain rule:

$$\psi_{xx} = \frac{\Psi_{bb}}{\Psi_{aa}\Psi_{bb} - \Psi_{ab}^2}, \quad \psi_{xy} = -\frac{\Psi_{ab}}{\Psi_{aa}\Psi_{bb} - \Psi_{ab}^2}, \quad \psi_{yy} = \frac{\Psi_{aa}}{\Psi_{aa}\Psi_{bb} - \Psi_{ab}^2}.$$

It is now a simple matter to transform (10), by making use of the above formulae and (14), to obtain the linear problem

$$\left(a^2 + \frac{b^2}{n}\right)\Psi_{aa} + 2\left(1 - \frac{1}{n}\right)ab\Psi_{ab} + \left(b^2 + \frac{a^2}{n}\right)\Psi_{bb} = 0. \tag{16}$$

The conditions on the free boundary (11) can be expressed in the form

$$N_1 a + N_2 b = 0, \quad N_1 b - N_2 a = N_1, \quad N_1^2 + N_2^2 = 1,$$

where $\boldsymbol{N} = (N_1, N_2)$ is the unit normal vector in the (a, b)-plane. We can therefore deduce that

$$N_1 = \frac{b}{(a^2 + b^2)^{1/2}}, \quad N_2 = -\frac{a}{(a^2 + b^2)^{1/2}},$$

and that the free boundary is represented, in the transformed plane, by the semicircle

$$\left(b - \frac{1}{2}\right)^2 + a^2 = \frac{1}{4}, \quad a \leqslant 0. \tag{17}$$

On (17) the condition $(11)_2$ can be expressed as

$$a\Psi_a + b\Psi_b - \Psi = \Psi_b. \tag{18}$$

By noting that (i) $\psi_x = 0$ along the top ($y = 1$) and midlines ($y = 0$) of the Hele-Shaw cell, (ii) $0 < \psi_y < \lambda$ on the top, and (iii) $\lambda < \psi_y \leqslant 1$ on the midline, the conditions (13) can be transformed to the boundary condition

$$\left.\begin{array}{ll} \Psi = 0 & \text{for} \quad 1 \geqslant b > \lambda \\ \Psi = b - \lambda & \text{for} \quad 0 < b < \lambda \end{array}\right\} \quad \text{on} \quad a = 0, \tag{19}$$

which closes the semicircular domain on which Ψ is to be calculated (see Fig. 2). The problem for Ψ, comprising (16), (18) and (19), is linear and on a prescribed domain. Note, however, that Ψ is determined only up to an arbitrary multiple of a, corresponding to the invariance of (10) to (13) under translations of x.

3.1 *Polar coordinates*

In order to effect an asymptotic solution, it proves helpful to introduce the coordinates (ρ, θ) defined (*cf.* (**13**)) by

$$a = -\rho \sin\theta, \quad b = \rho \cos\theta.$$

In terms of these, the problem for Ψ, comprised of (16), (18) and (19), transforms to

$$n\Psi_{\rho\rho} + \frac{1}{\rho}\Psi_\rho + \frac{1}{\rho^2}\Psi_{\theta\theta} = 0, \tag{20}$$

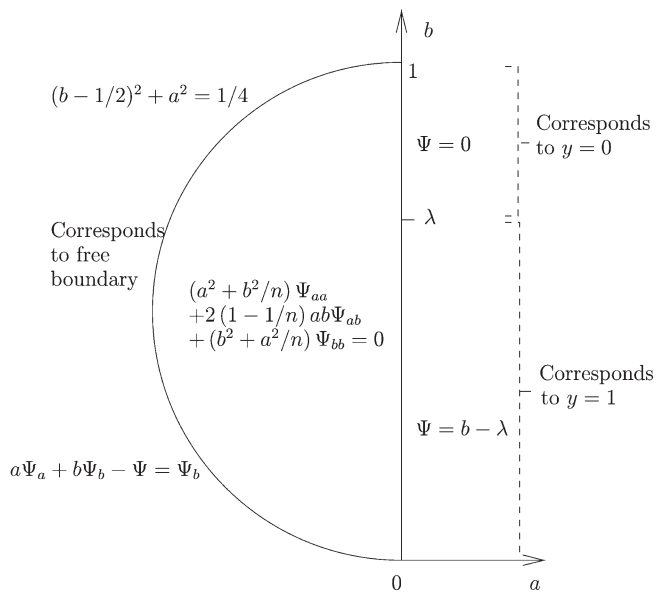

Fig. 2 The formulation in the Legendre plane

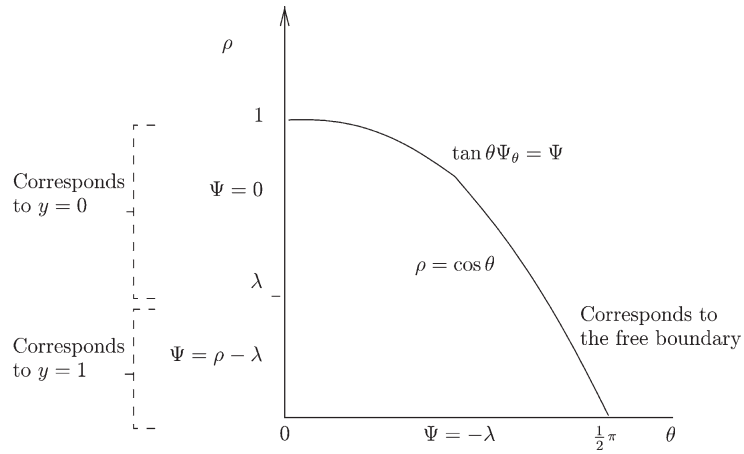

Fig. 3 The formulation in the Legendre plane (polar coordinates)

$$\tan\theta\Psi_\theta - \Psi = 0 \quad \text{on} \quad \rho = \cos\theta, \tag{21}$$

$$\left.\begin{array}{ll} \Psi = 0 & \text{for} \quad \lambda < \rho < 1 \\ \Psi = \rho - \lambda & \text{for} \quad 0 < \rho < \lambda \end{array}\right\} \quad \text{on} \quad \theta = 0, \tag{22}$$

$$\Psi = -\lambda \quad \text{for} \quad \rho = 0, \tag{23}$$

where the final condition is added at the singular point $\rho = 0$ in order to ensure a non-singular solution to the problem; the problem comprised of (20) to (23) determines Ψ uniquely up to an arbitrary multiple of $\rho\sin\theta$. The domain and boundary conditions are shown in Fig. 3

3.2 *Logarithmic transform*

Before determining an asymptotic solution to this system, we transform the equations a final time by introducing variables

$$q = -\log\rho, \quad \Psi = \lambda(e^{-q}\cos\theta - 1) + \exp\left(-\frac{1}{2}\left(1 - \frac{1}{n}\right)q\right)\chi(q,\theta). \tag{24}$$

Here the first term in Ψ (which corresponds to $(x, y) = (0, \lambda)$, $\psi = \lambda$ in physical variables) is chosen in order to subtract off the $O(1)$ term in the far-field solution ($q \to +\infty$) to reveal important exponentially-small terms in χ. Under the above transformation (20) to (23) is taken to an autonomous PDE (in effect the modified Helmholtz equation), namely

$$n\chi_{qq} + \chi_{\theta\theta} - \frac{n}{4}\left(1 - \frac{1}{n}\right)^2\chi = 0, \tag{25}$$

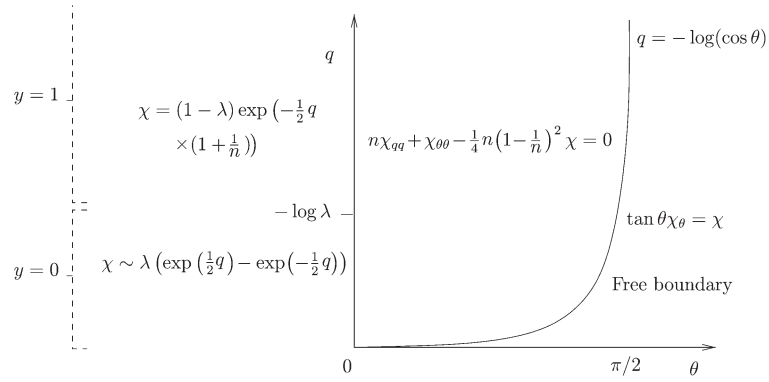

Fig. 4 The boundary-value problem after the logarithmic transform

with boundary conditions

$$\tan\theta\chi_\theta = \chi \quad \text{on} \quad q = -\log(\cos\theta), \tag{26}$$

$$\left.\begin{aligned} \chi &= \lambda\left(\exp\left(\frac{q}{2}\left(1-\frac{1}{n}\right)\right)-\exp\left(-\frac{q}{2}\left(1+\frac{1}{n}\right)\right)\right) && \text{for } 0 < q < \log\left(\frac{1}{\lambda}\right) \\ \chi &= (1-\lambda)\exp\left(-\tfrac{q}{2}\left(1+\tfrac{1}{n}\right)\right) && \text{for } \log\left(\frac{1}{\lambda}\right) < q < \infty \end{aligned}\right\} \text{on} \quad \theta = 0, \tag{27}$$

$$\chi \to 0 \quad \text{as} \quad q \to \infty. \tag{28}$$

The domain and boundary conditions are illustrated in Fig. 4; the problem comprised of (25) to (28) determines χ uniquely up to an arbitrary multiple of $\exp(-q(1+1/n)/2))\sin\theta$.

Once the solution for χ has been determined, the positions in physical space of points in the transformed plane, and the corresponding streamfunction ψ, can be found from (15); indeed, working backwards through the various transformations gives

$$x = \exp\left(\frac{q}{2}\left(1+\frac{1}{n}\right)\right)\left(\sin\theta\left(\chi_q-\frac{1}{2}\left(1-\frac{1}{n}\right)\chi\right)-\cos\theta\chi_\theta\right), \tag{29}$$

$$y = \lambda-\exp\left(\frac{q}{2}\left(1+\frac{1}{n}\right)\right)\left(\cos\theta\left(\chi_q-\frac{1}{2}\left(1-\frac{1}{n}\right)\chi\right)+\sin\theta\chi_\theta\right), \tag{30}$$

$$\psi = \lambda-\exp\left(-\frac{1}{2}\left(1-\frac{1}{n}\right)q\right)\left(\chi_q+\chi\left(\frac{1}{2}+\frac{1}{2n}\right)\right). \tag{31}$$

4. Asymptotic solution for ψ in the Legendre plane

4.1 *Region* I

4.1.1 *Solution to the leading-order problem.* In order to solve this problem asymptotically for large n (that is, in the strongly shear-thinning limit) we rescale about $\theta = 0$ and expand χ in powers

of $O(1/n)$ in the form

$$\theta = \frac{\Theta}{n^{1/2}}, \quad \chi = \chi_0^{(\mathrm{I})}(q,\Theta) + \frac{1}{n}\chi_1^{(\mathrm{I})}(q,\Theta) + \cdots .$$

In terms of this new variable, the leading-order problem for χ becomes the quarter-plane formulation

$$\frac{\partial^2 \chi_0^{(\mathrm{I})}}{\partial q^2} + \frac{\partial^2 \chi_0^{(\mathrm{I})}}{\partial \Theta^2} - \frac{\chi_0^{(\mathrm{I})}}{4} = 0, \tag{32}$$

$$\left.\begin{aligned} \chi_0^{(\mathrm{I})} &= 2\lambda \sinh\left(\frac{q}{2}\right) && \text{for } 0 < q < \log\left(\frac{1}{\lambda}\right) \\ \chi_0^{(\mathrm{I})} &= (1-\lambda)\exp\left(-\frac{q}{2}\right) && \text{for } \log\left(\frac{1}{\lambda}\right) < q \end{aligned}\right\} \quad \text{on} \quad \Theta = 0, \tag{33}$$

$$\chi_0^{(\mathrm{I})} \to 0 \quad \text{as} \quad q \to \infty, \tag{34}$$

$$\Theta \frac{\partial \chi_0^{(\mathrm{I})}}{\partial \Theta} - \chi_0^{(\mathrm{I})} = 0 \quad \text{on} \quad q = 0, \tag{35}$$

which here serves a role analogous to that of an inner-diffraction problem in the theory of geometrical optics and where the switch in boundary condition on $\Theta = 0$ corresponds to jumping from the centreline of the Hele-Shaw cell ($y = 0$) to the top boundary ($y = 1$) as q increases through $q = \log(1/\lambda)$. The problem (32) to (35) determines the solution $\chi_0^{(\mathrm{I})}$ up to an arbitrary multiple of $e^{-q/2}\Theta$ (corresponding to an arbitrary translation in x in the physical plane). Integrating (35) gives

$$\chi_0^{(\mathrm{I})} = B_0\Theta \quad \text{on} \quad q = 0, \tag{36}$$

where B_0 is an arbitrary constant. Specifying B_0 determines $\chi_0^{(\mathrm{I})}$ uniquely and hence determines the x coordinate of the finger tip in the physical plane at $O(n^{1/2})$ (the subsequent term is required to determine its position up to $O(1)$). Henceforth we shall take $B_0 = 0$ and replace the condition (35) by

$$\chi_0^{(\mathrm{I})}|_{q=0} = 0. \tag{37}$$

The problem comprised of (32) to (34) and (37) can be solved by use of a Fourier sine transform

$$\overline{\chi_0^{(\mathrm{I})}}(q,k) = \int_0^\infty \sin(k\Theta)\chi_0^{(\mathrm{I})}(q,\Theta)d\Theta, \quad \chi_0^{(\mathrm{I})}(q,\Theta) = \frac{2}{\pi}\int_0^\infty \sin(k\Theta)\,\overline{\chi_0^{(\mathrm{I})}}(q,k)dk \tag{38}$$

to give

$$\begin{aligned} \overline{\chi_0^{(\mathrm{I})}} = {} & \frac{(1-\lambda)e^{-q/2}}{k} + \frac{\lambda^{1/2}}{2k(k^2+1/4)^{1/2}}\left[\exp\left(-(k^2+1/4)^{1/2}(q-\log\lambda)\right)\right. \\ & \left. - \exp\left(-(k^2+1/4)^{1/2}(q+\log\lambda)\right)\right], \quad q \geqslant \log(1/\lambda), \\ \overline{\chi_0^{(\mathrm{I})}} = {} & \frac{\lambda(e^{q/2}-e^{-q/2})}{k} + \frac{\lambda^{1/2}}{2k(k^2+1/4)^{1/2}}\left[\exp\left(-(k^2+1/4)^{1/2}(q-\log\lambda)\right)\right. \\ & \left. - \exp\left((k^2+1/4)^{1/2}(q+\log\lambda)\right)\right], \quad q \leqslant \log(1/\lambda). \end{aligned}$$

Here we obtain different forms for $\chi_0^{(\mathrm{I})}$, depending on whether $q > \log(1/\lambda)$ or $q < \log(1/\lambda)$, as a result of the boundary condition switch in (33). Inversion is best accomplished by writing

$$\chi_0^{(\mathrm{I})}(q,\Theta) = \frac{2}{\pi}\Im\left(\int_0^\infty \exp(ik\Theta)\,\overline{\chi_0^{(\mathrm{I})}}(q,k)dk\right),$$

and then deforming the contour of integration to make a quarter turn round the pole at $k = 0$ and proceeding up the imaginary axis, so that

$$\chi_0^{(\mathrm{I})}(q,\Theta) = \Re\left(\mathrm{Res}\left(e^{ik\Theta}\overline{\chi_0^{(\mathrm{I})}}, k=0\right) + \frac{2}{\pi}\int_0^\infty e^{-\mu\Theta}\overline{\chi_0^{(\mathrm{I})}}(q,i\mu)d\mu\right). \tag{39}$$

Here $\Im(\cdot)$ and $\Re(\cdot)$ signify the imaginary and real parts of the argument, respectively. We note that the integrand in (39) is purely imaginary for $\mu \in [0, 1/2]$ and that the contribution from the pole at $k = 0$ is zero. It follows that (39) can be rewritten in terms of a real integral (with exponential decay):

$$\chi_0^{(\mathrm{I})} = \frac{2\lambda^{1/2}}{\pi}\int_{1/2}^\infty \frac{e^{-\mu\Theta}\sin\left((\mu^2-1/4)^{1/2}q\right)\sin\left((\mu^2-1/4)^{1/2}\log(1/\lambda)\right)}{\mu(\mu^2-1/4)^{1/2}}d\mu. \tag{40}$$

Leading-order approximations in the physical coordinates can be obtained from (29) to (31) and are, in this region,

$$x \sim -n^{1/2}\exp\left(\frac{q}{2}\right)\frac{\partial\chi_0^{(\mathrm{I})}}{\partial\Theta}, \qquad y \sim \lambda - \exp\left(\frac{q}{2}\right)\left(\frac{\partial\chi_0^{(\mathrm{I})}}{\partial q} - \frac{\chi_0^{(\mathrm{I})}}{2} + \Theta\frac{\partial\chi_0^{(\mathrm{I})}}{\partial\Theta}\right), \tag{41}$$

$$\psi \sim \lambda - \exp\left(-\frac{q}{2}\right)\left(\frac{\partial\chi_0^{(\mathrm{I})}}{\partial q} + \frac{\chi_0^{(\mathrm{I})}}{2}\right). \tag{42}$$

4.1.2 *The finger shape determined by the solution in region* I. On the line $q = 0$, corresponding to the finger boundary, we have $\chi_0^{(\mathrm{I})} = 0$; thus the expression $(42)_1$ for x is zero. A refined approximation of the free-boundary shape, obtained from (29), (30) and expansion of (40), and reflecting the fact that the boundary conditions are actually prescribed on q small but non-zero, is given by

$$x \sim \frac{1}{n^{1/2}}\left(\Theta\frac{\partial\chi_0^{(\mathrm{I})}}{\partial q} - \frac{\partial\chi_1^{(\mathrm{I})}}{\partial\Theta} - \frac{\Theta^2}{2}\frac{\partial^2\chi_0^{(\mathrm{I})}}{\partial\Theta\partial q}\right)\Bigg|_{q=0}, \tag{43}$$

$$y \sim \lambda - \frac{\partial\chi_0^{(\mathrm{I})}}{\partial q}\Bigg|_{q=0}; \tag{44}$$

here we use the observation that $\chi_0^{(\mathrm{I})}|_{q=0} = 0$. The value of $\chi_1^{(\mathrm{I})}|_{q=0}$ can be determined (without solving for $\chi_1^{(\mathrm{I})}$) from boundary condition (26), which in terms of the current variables can be written as

$$n^{1/2}\tan\left(\frac{\Theta}{n^{1/2}}\right)\frac{\partial\chi^{(\mathrm{I})}}{\partial\Theta} = \chi^{(\mathrm{I})} \quad \text{on} \quad q = -\log\left(\cos\left(\frac{\Theta}{n^{1/2}}\right)\right).$$

Substituting $\chi = \chi_0^{(\mathrm{I})} + \chi_1^{(\mathrm{I})}/n + \cdots$ into the above and expanding up to the $O(1)$ terms gives

$$\left(\Theta\frac{\partial\chi_1^{(\mathrm{I})}}{\partial\Theta} - \chi_1^{(\mathrm{I})}\right)\bigg|_{q=0} = \left\{\frac{1}{2}\left(\Theta^2\frac{\partial\chi_0^{(\mathrm{I})}}{\partial q} - \Theta^3\frac{\partial\chi_0^{(\mathrm{I})}}{\partial\Theta\partial q}\right) - \frac{\Theta^3}{3}\frac{\partial\chi_0^{(\mathrm{I})}}{\partial\Theta}\right\}\bigg|_{q=0}, \tag{45}$$

the last term of which is zero since $\chi_0^{(\mathrm{I})}|_{q=0} = 0$. Differentiating (45) with respect to Θ, dividing by Θ and integrating with respect to Θ gives the following expression for $\partial\chi_1^{(\mathrm{I})}/\partial\Theta|_{q=0}$:

$$\frac{\partial\chi_1^{(\mathrm{I})}}{\partial\Theta}\bigg|_{q=0} = \int_0^\Theta \frac{\partial\chi_0^{(\mathrm{I})}}{\partial q}\bigg|_{q=0} d\Theta - \frac{\Theta^2}{2}\frac{\partial^2\chi_0^{(\mathrm{I})}}{\partial q\partial\Theta}\bigg|_{q=0} + B_1, \tag{46}$$

where B_1 is an arbitrary constant (corresponding to a translation in x) which we set equal to zero, thus determining the $O(1)$ term in the expansion of the x-coordinate of the finger tip. Substituting (46) into (43), (44) and using the expression for $\chi_0^{(\mathrm{I})}$ in (40) gives the following parametrization for the leading edge of the finger:

$$x \sim \frac{2\lambda^{1/2}}{\pi n^{1/2}}\left(\Theta\frac{d\Omega}{d\Theta} - \Omega\right), \quad y \sim \lambda - \frac{2\lambda^{1/2}}{\pi}\frac{d\Omega}{d\Theta}, \tag{47}$$

where

$$\Omega(\Theta;\lambda) = -\int_{1/2}^{\infty} \frac{e^{-\mu\Theta}\sin\left((\mu^2 - 1/4)^{1/2}\log(1/\lambda)\right)}{\mu^2} d\mu. \tag{48}$$

Plots of the finger shape, found by evaluating these formulae numerically, are given in Fig. 7 for various values of λ.

Large-Θ asymptotic representations of (47) can be found by using Laplace's method on the integral in (48) to obtain

$$x \sim \frac{2\lambda^{1/2}\log(1/\lambda)}{n^{1/2}\pi^{1/2}}\frac{\exp(-\Theta/2)}{\Theta^{1/2}}, \quad y \sim \lambda - \frac{2\lambda^{1/2}\log(1/\lambda)}{\pi^{1/2}}\frac{\exp(-\Theta/2)}{\Theta^{3/2}} \quad \text{as} \quad \Theta \to +\infty.$$

This gives the matching behaviour for the finger shape to be determined, in section 4.3, by the solution in region III. As can be seen from Fig. 6, this corresponds in the physical plane to where the free boundary begins to 'turn the corner'.

4.1.3 *Far-field behaviour of* $\chi_0^{(\mathrm{I})}$. In order to determine the behaviour of χ in regions in which $\theta \gg n^{-1/2}$ and/or $q \gg 1$, it is first necessary to obtain the relevant matching conditions by analysis of $\chi_0^{(\mathrm{I})}$ as either or both $q \to \infty$ and $\Theta \to \infty$.

4.1.4 *Behaviour of* $\chi_0^{(\mathrm{I})}$ *as* $\Theta \to \infty$, $q = O(1)$. Applying Laplace's method to the integral in (40) yields the large-Θ behaviour

$$\chi_0^{(\mathrm{I})} \sim \frac{2\lambda^{1/2}\log(1/\lambda)qe^{-\Theta/2}}{\pi^{1/2}\Theta^{3/2}} + \cdots \quad \text{as} \quad \Theta \to +\infty, \ \ q = O(1), \tag{49}$$

where the dominant contribution to (40) comes from the end point $\mu = 1/2$ of the integral.

4.1.5 *Behaviour of $\chi_0^{(\mathrm{I})}$ as $\Theta \to +\infty$, $q = O(\Theta)$.* For the limit in which both Θ and q simultaneously tend to ∞ the process is more involved but can be calculated by deforming the contour of integration into the complex plane and integrating along the path of steepest descent. By making the substitution $\mu = s + 1/2$, the expression (40) can be rewritten as

$$\chi_0^{(\mathrm{I})} = \frac{2\lambda^{1/2}}{\pi} \exp\left(-\frac{\Theta}{2}\right) \Im\left[\int_0^\infty \exp(\Theta(-s + ih(s+s^2)^{1/2}) f(s) ds\right], \tag{50}$$

where

$$h = \frac{q}{\Theta}, \quad f(s) = \frac{\sin\left((s+s^2)^{1/2}\log(1/\lambda)\right)}{(s+1/2)(s+s^2)^{1/2}}. \tag{51}$$

We now consider the limit $\Theta \to +\infty$, $h = O(1)$. The steepest-descent contour is

$$-s + ih(s+s^2)^{1/2} = -\tau, \quad \tau \in \mathbb{R}, \quad \tau \geqslant 0,$$

and its relevant branch (plotted in Fig. 8(a)) is given by

$$s = \frac{(2\tau - h^2) + (h^4 - 4h^2(\tau+\tau^2))^{1/2}}{2(1+h^2)} \quad \text{for} \quad -\infty < \tau < 0$$

(note that $\tau = 0$ corresponds to $s = 0$). For $0 < \tau < ((1+h^2)^{1/2} - 1)/2$ we have that $s \in \mathbb{R}$ and there is no contribution to $\chi_0^{(\mathrm{I})}$ from the integral in (50), as the integrand is real. The major contribution to $\chi_0^{(\mathrm{I})}$ (an end-point contribution) thus comes from τ just greater than $\tau_2 = ((1+h^2)^{1/2} - 1)/2$; in terms of Fig. 8(a) this is just after the steepest-descent contour leaves the negative real axis at $s = -(1 - (1+h^2)^{-1/2})/2$. This suggests the substitution

$$\tau = \frac{(1+h^2)^{1/2} - 1}{2} + t.$$

For small t, we can approximate s in (50) by

$$s \sim -\frac{1}{2} + \frac{1}{2(1+h^2)^{1/2}} + ih(1+h^2)^{-3/4} t^{1/2} + \cdots,$$

and hence $\chi_0^{(\mathrm{I})}$ by

$$\chi_0^{(\mathrm{I})} \sim \frac{2\lambda^{1/2}}{\pi} \exp\left(-\frac{\Theta(1+h^2)^{1/2}}{2}\right)$$

$$\times \Re\left[\int_0^\infty \exp(-\Theta t) f\left(-\frac{1}{2} + \frac{1}{2(1+h^2)^{1/2}}\right) \frac{h(1+h^2)^{-3/4}}{2t^{1/2}} dt\right].$$

Evaluating the integral and substituting for h from (51) gives, as $q \to +\infty$ with $\Theta = O(q)$,

$$\chi_0^{(\mathrm{I})} \sim \frac{4\lambda^{1/2}}{\pi^{1/2}} \frac{(\Theta^2+q^2)^{1/4}}{\Theta} \sinh\left(\frac{q\log(1/\lambda)}{2(\Theta^2+q^2)^{1/2}}\right) \exp\left(-\frac{(q^2+\Theta^2)^{1/2}}{2}\right), \tag{52}$$

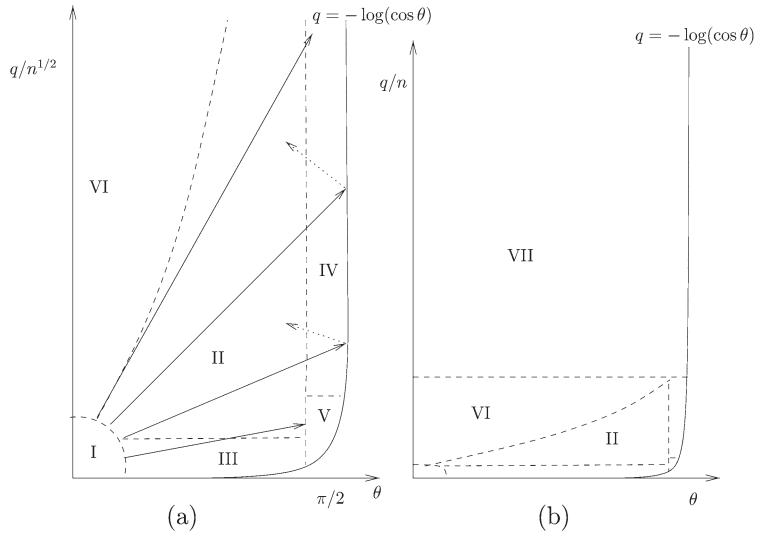

Fig. 5 The asymptotic regions in the Legendre plane (after logarithmic transform) in the limit $n \to \infty$. In (a) the solid arrows show the transmission of information along the rays of equation (56) from region I to regions IV and V. The dotted arrows represent the rays reflected from the boundary but, because the governing PDE (25) is the modified Helmholtz equation, the contributions of the reflected rays decay exponentially along their paths and are thus of importance only in region IV. In (b) the vertical axis has been compressed in order to show region VII

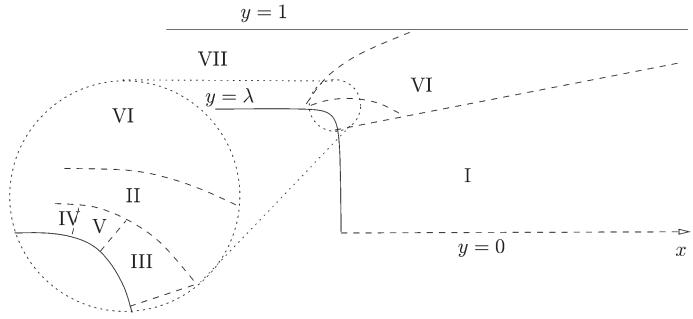

Fig. 6 A sketch of the asymptotic regions in the physical plane in the limit $n \to \infty$; compare with Fig. 5

wherein the preexponential factor corresponds (in analogy with canonical diffraction problems) to the directivity associated with the expansion fan emanating from this region (*cf.* Fig. 5(a)).

4.1.6 *Behaviour of* $\chi_0^{(\mathrm{I})}$ *as* $q \to +\infty$, $\Theta = O(q^{1/2})$. The above asymptotic formula for $\chi_0^{(\mathrm{I})}$ clearly does not hold all the way to the boundary $\Phi = 0$, on which $\chi_0^{(\mathrm{I})} = (1 - \lambda)\exp(-q/2)$, a

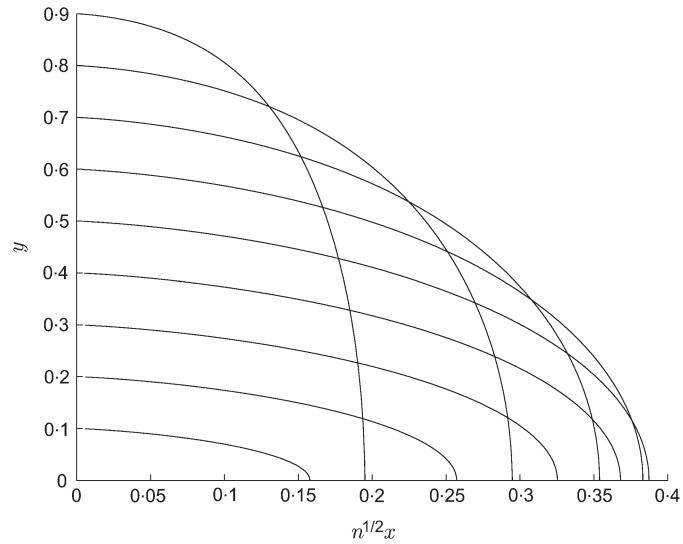

Fig. 7 The leading-order finger shape (in the physical plane), which is independent of n in the coordinates shown, determined by the solution in region I; this corresponds to the leading edge of the finger. Here we have, moving up the y-axis, $\lambda = 0{\cdot}1, 0{\cdot}2, \ldots, 0{\cdot}9$. The x origin has been fixed by the choices $B_0 = B_1 = 0$, leading here to the intersection of the finger with the x-axis varying non-monotonically with λ

different asymptotic behaviour arising where $q \to +\infty$ with $\Theta = O(q^{1/2})$. Here we again make the substitution $\mu = s + 1/2$ in (40) and rewrite $\chi_0^{(\mathrm{I})}$ in the form

$$\chi_0^{(\mathrm{I})} = \frac{2\lambda^{1/2}}{\pi} \Im \left[\int_0^\infty \exp(iq(s+s^2)^{1/2}) g(s) ds \right],$$

where

$$g(s) = \exp\left(-\Theta \left(s + \frac{1}{2} \right) \right) \frac{\sin\left((s+s^2)^{1/2} \log(1/\lambda) \right)}{(s+1/2)(s+s^2)^{1/2}}.$$

The steepest-descent contour is now given by $iq(s+s^2)^{1/2} = -\tau$, where τ is real and positive and is plotted in Fig. 8(b). It follows that

$$s = \frac{-1 + (1 - 4\tau^2/q^2)^{1/2}}{2}$$

(note that $\tau = 0$ corresponds to $s = 0$). For $0 \leqslant \tau < q/2$, s is real and negative and the integrand is real. It follows that there is no contribution to $\chi_0^{(\mathrm{I})}$ for $0 \leqslant \tau < q/2$. However, a contribution (equal to one-quarter of the residue) is picked up around the pole at $s = -1/2$, in addition to an end-point contribution from the line running up $\Re(s) = -1/2$; thus

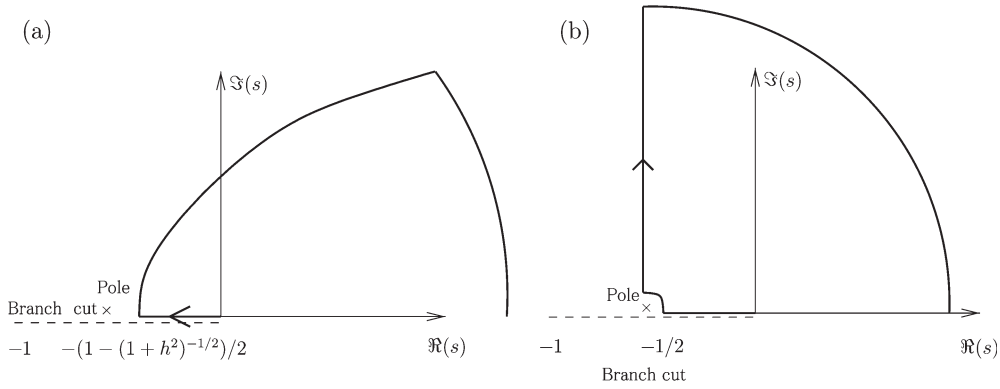

Fig. 8 The steepest-descent contours used for calculating the asymptotic behaviour of $\chi_0^{(\mathrm{I})}$. The dashed line is a branch cut running between the branch points at $s = 0$ and $s = -1$

$$\chi_0^{(\mathrm{I})} = \frac{2\lambda^{1/2}}{\pi}\Im\left[\frac{\pi i}{2}\mathrm{Res}\Big(\exp(iq(s+s^2)^{1/2})g(s), s=-1/2\Big)\right.$$

$$\left. + \int_{-1/2}^{-1/2+i\infty} \exp(iq(s+s^2)^{1/2})g(s)ds\right].$$

Evaluating the residue and making the substitution $s = -1/2 + i(t+t^2)^{1/2}$ gives

$$\chi_0^{(\mathrm{I})} = \frac{2\lambda^{1/2}e^{-q/2}}{\pi}\left[\pi\sinh\left(\frac{\log(1/\lambda)}{2}\right)\right.$$

$$\left. - \int_0^{\infty} \frac{\sin(\Theta(t+t^2)^{1/2})\sinh((t+t^2)^{1/2}\log(1/\lambda))}{(t+t^2)}e^{-qt}dt\right].$$

The integral in the above expression may be approximated in the limit $q \to +\infty$, $\Theta = O(q^{1/2})$ by writing $\Theta = q^{1/2}\gamma$, making the substitution $t = \tau/q$ and expanding in powers of q; this gives

$$\int_0^{\infty} \frac{\sin(\gamma q^{1/2}(t+t^2)^{1/2})\sinh((t+t^2)^{1/2}\log(1/\lambda))}{(t+t^2)}e^{-qt}dt$$

$$\sim \sinh\left(\frac{\log(1/\lambda)}{2}\right)\int_0^{\infty}\frac{\sin(\gamma\tau^{1/2})}{\tau}e^{-\tau}d\tau = \pi\sinh\left(\frac{\log(1/\lambda)}{2}\right)\mathrm{erf}\left(\frac{\gamma}{2}\right),$$

where $\mathrm{erf}(\cdot)$ is the error function. It follows that the asymptotic behaviour of $\chi_0^{(\mathrm{I})}$ is

$$\chi_0^{(\mathrm{I})} \sim (1-\lambda)e^{-q/2}\left(1-\mathrm{erf}\left(\frac{\Theta}{2q^{1/2}}\right)\right) \quad \text{as} \quad q\to\infty \quad \text{with} \quad \frac{\Theta}{q^{1/2}} = O(1). \tag{53}$$

Note that this expression satisfies the boundary condition $\chi_0^{(\mathrm{I})} = (1-\lambda)e^{-q/2}$ on $\Theta = 0$ and matches to the behaviour (52) as $\Theta/q^{1/2} \to \infty$. The leading-order solution (53) is of 'shadow-boundary' type, corresponding to the parabolic approximation to the modified Helmholtz equation. The presence of the various sublayers we have described in the far field of $\chi_0^{(\mathrm{I})}$ is reflected in the full asymptotic structure of the solutions in the limit $n \to \infty$ (*cf.* Fig. 5). We now proceed to discuss region II, into which the expansion fan solution (52) matches.

4.2 *Region* II

We look for a solution for $\chi = \chi^{(\mathrm{II})}(\tilde{q}, \theta)$, in a region in which $q = O(n^{1/2})$ and $\theta = O(1)$, by introducing the new coordinate $q = n^{1/2}\tilde{q}$. With this rescaling, equation (25) becomes

$$\frac{\partial^2 \chi^{(\mathrm{II})}}{\partial \tilde{q}^2} + \frac{\partial^2 \chi^{(\mathrm{II})}}{\partial \theta^2} - \frac{n}{4}\left(1 - \frac{1}{n}\right)^2 \chi^{(\mathrm{II})} = 0. \tag{54}$$

An asymptotic solution to this can be found by using a WKBJ ansatz

$$\chi^{(\mathrm{II})} = \frac{4\lambda^{1/2} n^{-1/4}}{\pi^{1/2}} \exp\left(n^{1/2} h_0(\tilde{q}, \theta)\right)\left(H_0(\tilde{q}, \theta) + \frac{1}{n^{1/2}} H_1(\tilde{q}, \theta) + \cdots\right). \tag{55}$$

To leading order this gives an Eikonal equation for h_0,

$$h_{0,\theta}^2 + h_{0,\tilde{q}}^2 = \frac{1}{4}. \tag{56}$$

Solving subject to initial conditions obtained by matching to (52) as $\tilde{q} \to 0$ and $\theta \to 0$ gives the expansion fan solution

$$h_0 = -\frac{\left(\tilde{q}^2 + \theta^2\right)^{1/2}}{2}.$$

Proceeding to next order in the expansion yields the amplitude equation

$$2\left(\theta H_{0,\theta} + \tilde{q} H_{0,\tilde{q}}\right) + H_0 = 0$$

for H_0, with general solution

$$H_0 = \theta^{-1/2} P\left(\frac{\tilde{q}}{\theta}\right),$$

where the 'directivity' $P(\cdot)$ is a function which is determined by matching with (52) as $\tilde{q} \to 0$ and $\theta \to 0$, so that

$$H_0(\tilde{q}, \theta) = \frac{4\lambda^{1/2} n^{-1/4}}{\pi^{1/2}}\left[\frac{(\theta^2 + \tilde{q}^2)^{1/4}}{\theta} \sinh\left(\frac{1}{2}\frac{\tilde{q}\log(1/\lambda)}{(\tilde{q}^2 + \theta^2)^{1/2}}\right)\right], \tag{57}$$

from which we deduce that the WKBJ ansatz (55) gives the following asymptotic formula for $\chi^{(\mathrm{II})}$ as $n \to \infty$:

$$\chi^{(\mathrm{II})} \sim \frac{4\lambda^{1/2} n^{-1/4}}{\pi^{1/2}}\left[\frac{(\theta^2 + \tilde{q}^2)^{1/4}}{\theta} \sinh\left(\frac{1}{2}\frac{\tilde{q}\log(1/\lambda)}{(\tilde{q}^2 + \theta^2)^{1/2}}\right) + O\left(n^{-1/2}\right)\right]$$

$$\times \exp\left(-n^{1/2}\frac{(\tilde{q}^2 + \theta^2)^{1/2}}{2}\right). \tag{58}$$

Note that this solution does not satisfy the boundary condition (26) on $\theta \sim \pi/2 - \exp(-n^{1/2}\tilde{q})$ (that is, on $q = \log(\cos\theta)$) and it will therefore be necessary to introduce a further region in the vicinity of the boundary (namely region IV).

Physical coordinates may be found by substituting the solution ansatz (55) into (29) to (31); this gives

$$\begin{aligned} x &\sim \frac{2\lambda^{1/2}n^{1/4}}{\pi^{1/2}} \exp\left(-\frac{n^{1/2}}{2}((\tilde{q}^2+\theta^2)^{1/2}-\tilde{q})\right) \frac{\theta}{(\tilde{q}^2+\theta^2)^{1/2}} \cos\theta H_0(\tilde{q},\theta), \\ y &\sim \lambda + \frac{2\lambda^{1/2}n^{1/4}}{\pi^{1/2}} \exp\left(-\frac{n^{1/2}}{2}((\tilde{q}^2+\theta^2)^{1/2}-\tilde{q})\right) \frac{\theta}{(\tilde{q}^2+\theta^2)^{1/2}} \sin\theta H_0(\tilde{q},\theta), \\ \psi &\sim \lambda - \frac{2\lambda^{1/2}n^{-1/4}}{\pi^{1/2}} \exp\left(-\frac{n^{1/2}}{2}((\tilde{q}^2+\theta^2)^{1/2}+\tilde{q})\right) \left(1-\frac{\tilde{q}}{(\tilde{q}^2+\theta^2)^{1/2}}\right) H_0(\tilde{q},\theta), \end{aligned} \tag{59}$$

where H_0 is given by (57). Rewriting these in terms of the radial coordinates $r = (x^2+(y-\lambda)^2)^{1/2}$ and $\phi = \arctan((y-\lambda)/x)$ gives

$$\begin{gathered} r \sim \frac{2\lambda^{1/2}n^{1/4}}{\pi^{1/2}} \exp\left(-\frac{n^{1/2}}{2}((\tilde{q}^2+\theta^2)^{1/2}-\tilde{q})\right) \frac{\theta}{(\tilde{q}^2+\theta^2)^{1/2}} H_0(\tilde{q},\theta), \qquad \phi \sim \theta, \\ \log(\lambda-\psi) \sim -\frac{n\phi^2}{4\log(1/r)}. \end{gathered} \tag{60}$$

4.3 *Region* III

4.3.1 *Leading-order solution.* We now look for an asymptotic solution to (25), (26) in the region in which both q and θ are $O(1)$ by making the WKBJ ansatz

$$\chi^{(\mathrm{III})}(q,\theta) \sim \frac{2\lambda^{1/2}\log(1/\lambda)n^{-3/4}}{\pi^{1/2}} \exp\left(-n^{1/2}\frac{\theta}{2}\right)\left(G_0(q,\theta)+n^{-1/2}G_1(q,\theta)+\cdots\right). \tag{61}$$

Here the dominant behaviour $\log(\chi^{(\mathrm{III})}) \sim -n^{1/2}\theta/2$ is a consequence of matching $\chi^{(\mathrm{III})}$, in the limit $q \to \infty$, to $\chi^{(\mathrm{II})}$. To next order this ansatz gives

$$G_{0,qq} = 0 \Longrightarrow G_0 = \mathcal{A}(\theta)q + \mathcal{B}(\theta),$$

the reason for this trivial balance being that the region is essentially a passive one, required simply to moderate the ray solution in order to fit the boundary conditions (the boundary is perturbed from $q = 0$ by an amount that is asymptotically much smaller than the q scaling corresponding to the parabolic approximation). Here $\mathcal{A}(\cdot)$ and $\mathcal{B}(\cdot)$ are functions that are determined by matching to region II in the limit $q \to \infty$ and applying the boundary condition (26) on $q = -\log(\cos(\theta))$ (which gives $\mathcal{A}(\theta)q + \mathcal{B}(\theta)|_{q=-\log(\cos(\theta))} = 0$), so that

$$G_0(q,\theta) = \frac{q+\log(\cos\theta)}{\theta^{3/2}}. \tag{62}$$

Substitution of G_0 back into (61) implies that

$$\chi^{(\mathrm{III})} \sim \frac{2\lambda^{1/2}\log(1/\lambda)n^{-3/4}}{\pi^{1/2}}\left(\frac{q+\log(\cos\theta)}{\theta^{3/2}} + n^{-1/2}G_1(q,\theta) + \cdots\right)\exp\left(-n^{1/2}\frac{\theta}{2}\right). \quad (63)$$

The correction term $n^{-1/2}G_1(q,\theta)$ is included here because it appears in the calculation of the finger shape and needs (for this purpose) to be evaluated on $q = -\log(\cos\theta)$, but not elsewhere. Proceeding to first order in the expansion of (26) gives

$$\tan\theta\left(G_{0,\theta} - \frac{G_1}{2}\right) = G_0 \qquad \text{on} \quad q = -\log(\cos\theta),$$

from which it follows that

$$G_1|_{q=-\log(\cos(\theta))} = -\frac{2\tan\theta}{\theta^{3/2}}. \quad (64)$$

The physical quantities may be found by substituting the solution ansatz (61) into (29) to (31); this gives

$$\begin{aligned} x &\sim \frac{\lambda^{1/2}\log(1/\lambda)n^{-1/4}}{\pi^{1/2}}\exp\left(-\frac{n^{1/2}}{2}\theta\right)G_0 e^{q/2}\cos\theta, \\ y &\sim \lambda + \frac{\lambda^{1/2}\log(1/\lambda)n^{-1/4}}{\pi^{1/2}}\exp\left(-\frac{n^{1/2}}{2}\theta\right)G_0 e^{q/2}\sin\theta, \\ \psi &\sim \lambda - \frac{2\lambda^{1/2}\log(1/\lambda)n^{-3/4}}{\pi^{1/2}}\exp\left(-\frac{n^{1/2}}{2}\theta\right)e^{-q/2}\left(G_{0,q} + \frac{G_0}{2}\right), \end{aligned} \quad (65)$$

where G_0 is given by equation (62). Again rewriting these in terms of the radial coordinates $r = (x^2 + (y-\lambda)^2)^{1/2}$ and $\phi = \arctan((y-\lambda)/x)$ gives

$$\begin{gathered} r \sim \frac{\lambda^{1/2}\log(1/\lambda)n^{-1/4}}{\pi^{1/2}}\exp\left(-\frac{n^{1/2}}{2}\theta\right)G_0 e^{q/2}, \qquad \phi \sim \theta, \\ \log(\lambda - \psi) \sim -\frac{n^{1/2}}{2}\phi. \end{gathered} \quad (66)$$

4.3.2 *Finger shape determined by the solution in region* III. The leading edge of the finger (as determined by the solution in region I) is almost flat, lying approximately parallel to the y-axis. The shape of the finger as it rounds the 'corner', away from the vertical, is determined by expanding the solution in region III in powers of n along $q = -\log(\cos(\theta))$, and substitution into equations (29), (30). To the relevant orders this gives the following expressions for $x(\theta)$ and $y(\theta)$:

$$x \sim \frac{2\lambda^{1/2}\log(1/\lambda)n^{-3/4}}{\pi^{1/2}}\exp\left(-n^{1/2}\frac{\theta}{2}\right)(\cos\theta)^{-1/2}\left(2\frac{\sin\theta}{\theta^{3/2}} + \frac{\cos\theta}{2}G_1(q,\theta)\right)\Bigg|_{q=-\log(\cos(\theta))},$$

$$y \sim \lambda - \frac{2\lambda^{1/2}\log(1/\lambda)n^{-3/4}}{\pi^{1/2}} \times \exp\left(-n^{1/2}\frac{\theta}{2}\right)(\cos\theta)^{-1/2}\left(\frac{\sec\theta}{\theta^{3/2}} + \frac{\sin\theta}{2}G_1(q,\theta)\right)\Bigg|_{q=-\log(\cos(\theta))}.$$

Substituting for $G_1|_{q=-\log(\cos\theta)}$, using (64), gives the finger shape parametrized by θ

$$x \sim \frac{2\lambda^{1/2}\log(1/\lambda)n^{-3/4}}{\pi^{1/2}}\frac{\sin\theta}{\theta^{3/2}(\cos\theta)^{1/2}}\exp\left(-n^{1/2}\frac{\theta}{2}\right), \tag{67}$$

$$y \sim \lambda - \frac{2\lambda^{1/2}\log(1/\lambda)n^{-3/4}}{\pi^{1/2}}\frac{(\cos\theta)^{1/2}}{\theta^{3/2}}\exp\left(-n^{1/2}\frac{\theta}{2}\right). \tag{68}$$

The finger shape is plotted, for $\lambda = 0{\cdot}4$ and $n = 10$ and $n = 100$, in Fig. 9.

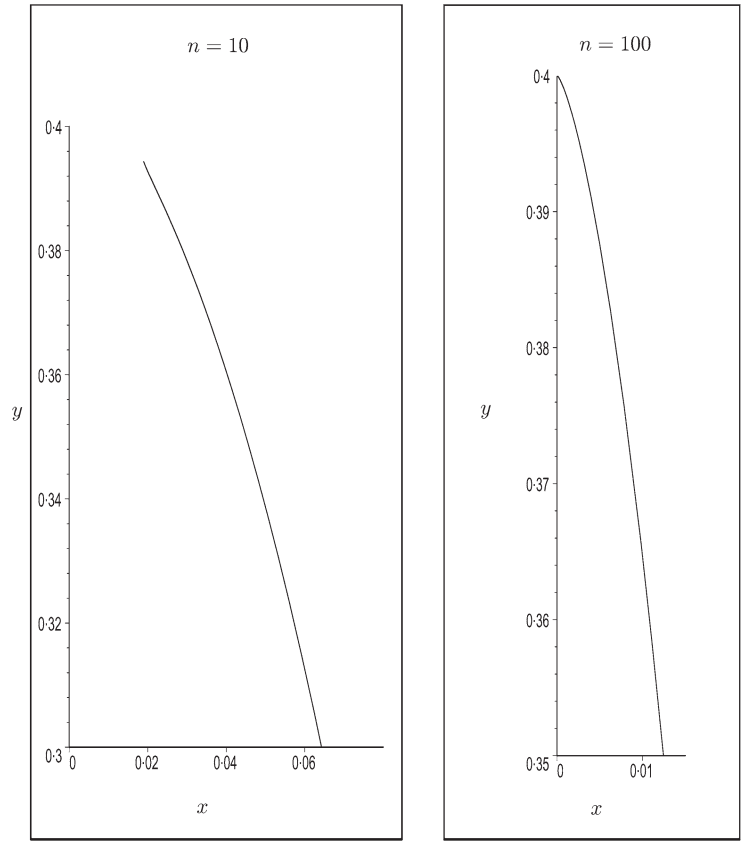

Fig. 9 The free boundary approaching the corner (with $\lambda = 0{\cdot}4$) as determined by the solution in region III. We note that the asymptotic expansion breaks down as $\theta \nearrow \pi/2$, with $(\cos\theta)^{-1/2}$ becoming comparable to $\exp(n^{1/2}\theta)$. We remark that (67), (68) depend explicitly on n, one consequence of this being that y is not single-valued as a function of x; we plot only the part of the curves which is asymptotically relevant. Note that the lower sections of the curves plotted here match to the upper section of the curve (with $\lambda = 0{\cdot}4$) from region I, as shown in Fig. 7. The upper sections of the curves here match the lower sections of those obtained from region V (which we cannot easily calculate because the problem is elliptic)

4.4 *Region* IV

As already noted, the asymptotic solution for χ in region II (namely $\chi^{(\mathrm{II})}$) does not satisfy the boundary condition (26). In region IV, shown schematically in Fig. 5, this manifests itself in a different way from in region III and thus needs separate discussion. Thus we introduce a further region in the vicinity of the boundary $q = -\log(\cos\theta)$ defined by the variables

$$\theta = \frac{\pi}{2} + \frac{\nu}{n^{1/2}}, \quad q = n^{1/2}\tilde{q}, \quad \chi = \chi^{(\mathrm{IV})}(\tilde{q}, \nu).$$

In terms of these new variables the boundary is approximated by $\nu \sim -n^{1/2}\exp(-n^{1/2}\tilde{q})$ and $\chi^{(\mathrm{IV})}$ satisfies

$$\frac{\partial^2\chi^{(\mathrm{IV})}}{\partial\nu^2} - \frac{1}{4}\left(1 - \frac{1}{n}\right)^2\chi^{(\mathrm{IV})} + \frac{1}{n}\frac{\partial^2\chi^{(\mathrm{IV})}}{\partial\tilde{q}^2} = 0 \quad \text{for } \nu < -n^{1/2}\exp(-n^{1/2}\tilde{q}) + \cdots, \tag{69}$$

$$\chi^{(\mathrm{IV})} + n^{1/2}\cot\left(\frac{\nu}{n^{1/2}}\right)\frac{\partial\chi^{(\mathrm{IV})}}{\partial\nu} = 0 \quad \text{on } \nu = -n^{1/2}\exp(-n^{1/2}\tilde{q}) + \cdots. \tag{70}$$

An approximate solution to this system can be obtained by making the WKBJ ansatz

$$\chi^{(\mathrm{IV})} = \frac{16\lambda^{1/2}n^{-1/4}}{\pi^{3/2}}\left(W_0(\tilde{q}, \nu) + n^{-1/2}W_1(\tilde{q}, \nu) + \cdots\right)\exp(-n^{1/2}w_0(\tilde{q})). \tag{71}$$

Matching to region II in the limit $\nu \to -\infty$ gives $w_0(\tilde{q}) = -\frac{1}{2}(\tilde{q}^2 + \pi^2/4)^{1/2}$. Substituting $\chi^{(\mathrm{IV})}$ into (69), (70) and taking the leading-order term gives the following equation and boundary condition for W_0:

$$W_{0,\nu\nu} - \frac{1}{16}\left(\frac{\pi^2}{(\tilde{q}^2 + \pi^2/4)^{1/2}}\right)W_0 = 0, \quad \text{and} \quad W_{0,\nu}|_{\nu=0} = 0,$$

with solution

$$W_0 = \mathcal{D}(\tilde{q})\cosh\left(\frac{\pi\nu}{4(\pi^2/4 + \tilde{q}^2)^{1/2}}\right). \tag{72}$$

Here $\mathcal{D}(\cdot)$ is a directivity which is determined by matching to the solution in region II in the limit $\nu \to -\infty$. Proceeding with the matching (in order to determine $\mathcal{D}$) and substituting the result, together with the expression for $w_0(\tilde{q})$, back into the ansatz for $\chi^{(\mathrm{IV})}$ gives the following asymptotic formula for $\chi^{(\mathrm{IV})}$ as $n \to \infty$:

$$\chi^{(\mathrm{IV})} \sim \frac{16\lambda^{1/2}n^{-1/4}}{\pi^{3/2}}\exp\left(-n^{1/2}\frac{(\tilde{q}^2 + \pi^2/4)^{1/2}}{2}\right)(\tilde{q}^2 + \pi^2/4)^{1/4}$$
$$\times \sinh\left(\frac{1}{2}\frac{\tilde{q}\log(1/\lambda)}{(\tilde{q}^2 + \pi^2/4)^{1/2}}\right)\cosh\left(\frac{\pi\nu}{4(\tilde{q}^2 + \pi^2/4)^{1/2}}\right). \tag{73}$$

Here the final cosh factor in this expression has a decaying exponential, as $\nu \to -\infty$, which leads to an exponentially small correction term to the solution in region II. The free-boundary shape given by (73) is simply $y \sim \lambda$ (up to the order of accuracy of this solution).

Again physical coordinates may be found by substituting the solution ansatz (61) into (29) to (31). In this case we find

$$\begin{aligned} x &\sim \frac{16\lambda^{1/2}}{\pi^{3/2}} n^{-1/4} \exp\left(-\frac{n^{1/2}}{2}\left(\left(\tilde{q}^2+\frac{\pi^2}{4}\right)^{1/2}-\tilde{q}\right)\right) \\ &\quad \times \left(\nu W_{0,\nu} - \frac{1}{2}\left(1+\frac{\tilde{q}}{(\tilde{q}^2+\pi^2/4)^{1/2}}\right) W_0\right), \\ y &\sim \lambda - \frac{16\lambda^{1/2}}{\pi^{3/2}} n^{1/4} \exp\left(-\frac{n^{1/2}}{2}\left(\left(\tilde{q}^2+\frac{\pi^2}{4}\right)^{1/2}-\tilde{q}\right)\right) W_{0,\nu}, \\ \psi &\sim \lambda - \frac{8\lambda^{1/2}}{\pi^{3/2}} n^{-1/4} \exp\left(-\frac{n^{1/2}}{2}\left(\left(\tilde{q}^2+\frac{\pi^2}{4}\right)^{1/2}+\tilde{q}\right)\right)\left(1-\frac{\tilde{q}}{(\tilde{q}^2+\pi^2/4)^{1/2}}\right) W_0, \end{aligned} \tag{74}$$

where W_0 is given by (72).

4.5 *Region* V (*the corner region*)

This corresponds to a second inner diffraction problem and gives the most difficult leading-order balance. However, because the rays that emerge from this region carry exponentially small contributions to the solution elsewhere, this need not trouble us unduly (though see section 6 for some pertinent remarks). Here we introduce the scaled variables

$$\theta = \frac{\pi}{2} + \frac{\nu}{n^{1/2}}, \quad q = \frac{1}{2}\log n + s, \quad \chi = \chi^{(V)}(s,\nu), \tag{75}$$

in terms of which equation (25) and boundary condition (26) can be rewritten as

$$n\left(\frac{\partial^2\chi^{(V)}}{\partial s^2} + \frac{\partial^2\chi^{(V)}}{\partial \nu^2} - \frac{\chi^{(V)}}{4}\right) + \frac{\chi^{(V)}}{2} - \frac{\chi^{(V)}}{4n} = 0, \tag{76}$$

$$\chi^{(V)} + n^{1/2}\cot\left(\frac{\nu}{n^{1/2}}\right)\frac{\partial\chi^{(V)}}{\partial\nu} = 0 \quad \text{on } \nu = -e^{-s}. \tag{77}$$

Matching to regions II, III and IV respectively gives far-field conditions on $\chi^{(V)}$:

$$\chi^{(V)} \sim \mathcal{P}(n,\lambda)e^{-\nu/2}\left(\frac{1}{2}\log n + s\right) \qquad \text{as } \nu\to-\infty \quad s\to+\infty \quad (s = O(\nu)), \tag{78}$$

$$\chi^{(V)} \sim \mathcal{P}(n,\lambda)e^{-\nu/2}(\log(-\nu)+s) \qquad \text{as } \nu\to-\infty \quad s\to-\infty \quad (s = O(\log(-\nu))), \tag{79}$$

$$\chi^{(V)} \sim \mathcal{P}(n,\lambda)\left(2\cosh\left(\frac{\nu}{2}\right)\left(\frac{1}{2}\log n + s\right)\right) \qquad \text{as } s\to+\infty \quad (\nu = O(1)), \tag{80}$$

where $\mathcal{P}$ is an exponentially small quantity defined by

$$\mathcal{P}(n,\lambda) = \left(\frac{4\sqrt{2}\lambda^{1/2}\log(1/\lambda)}{\pi^2}\right) n^{-3/4}\exp\left(-n^{1/2}\frac{\pi}{4}\right). \tag{81}$$

The expansion for $\chi^{(V)}$ thus proceeds in the form

$$\chi^{(V)} \equiv \mathcal{P}(n,\lambda)\left(\log n\chi_0^{(V)} + \chi_1^{(V)} + \cdots\right). \tag{82}$$

The first two terms satisfy

$$\frac{\partial^2\chi_0^{(V)}}{\partial s^2} + \frac{\partial^2\chi_0^{(V)}}{\partial \nu^2} - \frac{\chi_0^{(V)}}{4} = 0, \qquad \left.\frac{\partial\chi_0^{(V)}}{\partial\nu}\right|_{\nu=-e^{-s}} = 0, \tag{83}$$

$$\chi_0^{(V)} \to 0 \qquad \text{as } \nu\to-\infty, \quad s\to-\infty \quad (s = O(\log(-\nu))),$$

$$\chi_0^{(V)} \sim \frac{e^{-\nu/2}}{2} \qquad \text{as } \nu\to-\infty, \quad s\to+\infty \quad (s = O(\nu)),$$

$$\chi_0^{(V)} \sim \cosh\left(\frac{\nu}{2}\right) \qquad \text{as } s\to\infty \quad (\nu = O(1));$$

$$\frac{\partial^2\chi_1^{(V)}}{\partial s^2} + \frac{\partial^2\chi_1^{(V)}}{\partial \nu^2} - \frac{\chi_1^{(V)}}{4} = 0, \qquad \left.\frac{\partial\chi_1^{(V)}}{\partial\nu}\right|_{\nu=-e^{-s}} = 0,$$

$$\chi_1^{(V)} \sim e^{-\nu/2}(\log(-\nu)+s) \qquad \text{as } \nu\to-\infty, \quad s\to-\infty \quad (s = O(\log(-\nu))),$$

$$\chi_1^{(V)} \sim se^{-\nu/2} \qquad \text{as } \nu\to-\infty, \quad s\to+\infty \quad (s = O(\nu)),$$

$$\chi_1^{(V)} \sim 2s\cosh\left(\frac{\nu}{2}\right) \qquad \text{as } s\to+\infty \quad (\nu = O(1)). \tag{84}$$

These two problems require the solution of a linear elliptic PDE on a non-separable domain; they are unlikely to be amenable to standard analytical techniques. Note, however, that the problems for $\chi_0^{(V)}$ and $\chi_1^{(V)}$ are canonical—that is, they do not depend upon either λ or n.

The physical quantities in this regime are found by substituting the solution ansatz (75) and (82) into (29) to (31), to give

$$x \sim \mathcal{P}(n,\lambda)n^{1/4}\log ne^{s/2}\left(\frac{\partial\chi_0^{(V)}}{\partial s} - \frac{\chi_0^{(V)}}{2} + \nu\frac{\partial\chi_0^{(V)}}{\partial\nu}\right),$$

$$y \sim \lambda - \mathcal{P}(n,\lambda)n^{3/4}\log ne^{s/2}\frac{\partial\chi_0^{(V)}}{\partial\nu}, \tag{85}$$

$$\psi \sim \lambda - \mathcal{P}(n,\lambda)n^{-1/4}\log ne^{-s/2}\left(\frac{\partial\chi_0^{(V)}}{\partial s} + \frac{\chi_0^{(V)}}{2}\right),$$

where $\mathcal{P}(n,\lambda)$ is given in (81). It is noteworthy that the curvature of the free boundary calculated from the solution in region III increases as θ increases towards $\pi/2$; on the other hand, the free-boundary shape calculated from the solution in region IV is, to leading order, flat. It follows that for $\lambda = O(1)$ the curvature of the free boundary in the limit $n\to\infty$ is maximal in the region presently under discussion (which lies between III and IV), being of $O(\exp(n^{1/2}\pi/4)/[\lambda^{1/2}\log(1/\lambda)\log n])$. Thus the first part of the free boundary to be influenced when a small surface tension is introduced to the problem would naively be thought to be that described by the solution in region V.

4.6 *Region* VI

The differing asymptotic behaviours of $\chi_0^{(\mathrm{I})}$ as $q \to +\infty$ with (i) $\Theta = O(q)$ (see (52)), and (ii) with $\Theta = O(q^{1/2})$ (see (53)) suggest that $\chi_0^{(\mathrm{I})}$ matches, as $q \to +\infty$, to different asymptotic regions in which either (i) $n^{1/2}\theta = O(q)$, as in region II, or (ii) $n^{1/2}\theta = O(q^{1/2})$. Here we treat the latter case, the former being treated in section 4.2, by introducing the scaled coordinates

$$q = n^{1/2}\tilde{q}, \quad \theta = n^{-1/4}\tilde{\theta},$$

in terms of which the governing equation (25) and boundary condition $(27)_2$ are

$$\frac{\partial^2 \chi^{(\mathrm{VI})}}{\partial \tilde{q}^2} + n^{1/2}\frac{\partial^2 \chi^{(\mathrm{VI})}}{\partial \tilde{\theta}^2} - \frac{n}{4}\left(1 - \frac{1}{n}\right)^2 \chi^{(\mathrm{VI})} = 0, \tag{86}$$

$$\chi^{(\mathrm{VI})}|_{\theta=0} \sim (1-\lambda)\exp\left(-n^{1/2}\frac{\tilde{q}}{2}\left(1+\frac{1}{n}\right)\right). \tag{87}$$

As $\tilde{\theta} \to +\infty$ and as $\tilde{q} \to 0$ two further conditions can be obtained by matching to region II and region I (via (53)); these are, respectively

$$\chi^{(\mathrm{VI})} \sim \frac{2}{\pi^{1/2}}(1-\lambda)\frac{\tilde{q}^{1/2}}{\tilde{\theta}}\exp\left(-\frac{\tilde{\theta}^2}{4\tilde{q}}\right)\exp\left(-\frac{n^{1/2}\tilde{q}}{2}\right) \qquad \text{as } \tilde{\theta} \to \infty,$$

$$\chi^{(\mathrm{VI})} \sim (1-\lambda)\exp\left(-\frac{n^{1/2}\tilde{q}}{2}\right)\left(1 - \operatorname{erf}\left(\frac{\tilde{\theta}}{2\tilde{q}^{1/2}}\right)\right) \quad \text{as } \tilde{q} \to 0 \quad \text{with} \quad \tilde{\theta} = O(\tilde{q}^{1/2}).$$

Making the WKBJ ansatz

$$\chi^{(\mathrm{VI})} = \left(f_0(\tilde{q},\tilde{\theta}) + \frac{1}{n^{1/2}}f_1(\tilde{q},\tilde{\theta}) + \cdots\right)\exp\left(-\frac{n^{1/2}\tilde{q}}{2}\right)$$

and substituting into (86) to (88) leads to the following initial-value problem for f_0 (corresponding to the parabolic approximation in diffraction theory):

$$f_{0,\tilde{q}} = f_{0,\tilde{\theta}\tilde{\theta}},$$

$$f_0|_{\tilde{q}=0} = 0, \qquad f_0|_{\tilde{\theta}=0} = (1-\lambda), \qquad f_0 \to 0 \quad \text{as } \tilde{\theta} \to \infty,$$

with solution

$$f_0 = (1-\lambda)\left(1 - \operatorname{erf}\left(\frac{\tilde{\theta}}{2\tilde{q}^{1/2}}\right)\right)$$

(*cf.* a shadow boundary in diffraction theory) so that

$$\chi^{(\mathrm{VI})} \sim (1-\lambda)\exp\left(-\frac{n^{1/2}\tilde{q}}{2}\right)\left(1 - \operatorname{erf}\left(\frac{\tilde{\theta}}{2\tilde{q}^{1/2}}\right)\right). \tag{88}$$

Physical quantities may be found by substituting the solution ansatz (61) into (29) to (31). In this case we find

$$x = -n^{1/4} f_{0,\tilde{\theta}} + O(n^{-1/4}), \quad y = \lambda + (f_0 - \tilde{\theta} f_{0,\tilde{\theta}}) + O(n^{-1/2}), \tag{89}$$

$$\psi \sim \lambda - n^{-1/2} \exp(-n^{1/2}\tilde{q})(f_{0,\tilde{q}} + O(n^{-1/2})), \tag{90}$$

and approximate streamlines have constant $\tilde{q}$ and are shown in Fig. 10. Substituting for f_0 in the above we obtain

$$\frac{x}{n^{1/4}} = \frac{(1-\lambda)}{\pi^{1/2}} \frac{\exp(-\eta^2)}{\tilde{q}^{1/2}} + O(n^{-1/2}), \quad y = 1 + (1-\lambda)\left(\frac{2}{\pi^{1/2}}\eta \exp(-\eta^2) - \operatorname{erf}(\eta)\right),$$

$$\log\left(n^{1/2}(\lambda - \psi)\right) = -n^{1/2}\tilde{q} + O(1),$$

where $\eta = \tilde{\theta}/(2\tilde{q})$. It is apparent that, to leading order, y is a function of η only. Hence, if we introduce a function H defined by

$$H(y_0(\eta)) = \frac{(1-\lambda)^2}{\pi} \exp(-2\eta^2), \quad y_0 = 1 + (1-\lambda)\left(\frac{2}{\pi^{1/2}}\eta \exp(-\eta^2) - \operatorname{erf}(\eta)\right),$$

where $y_0(\eta)$ is the leading term in the expansion of y, we obtain

$$\log(n^{1/2}(\lambda - \psi)) \sim -n^{1/2}\frac{H(y)}{\xi^2}, \tag{91}$$

where $\xi = x/n^{(1/4)}$. Note that $y_0 \to \lambda^+$ as $\eta \to +\infty$ and that $y_0 = 1$ at $\eta = 0$. Furthermore, although H does not tend to infinity as $y \to 1^-$ its derivative dH/dy does. The fact that H remains finite on $y = 1$ despite the exact boundary condition being $\psi|_{y=1} = 0$ is indicative of the existence of an additional boundary layer (about $y = 1$) in the physical plane.

4.7 *Region* VII

Finally, we consider an extension of region VI, that is influenced directly by the finger boundary $q = -\log(\cos\theta)$, and the channel wall $\theta = 0$ by introducing the scaled coordinate

$$q = nQ.$$

In terms of Q the governing equation (25) and boundary conditions (27), (28) are

$$\frac{1}{n}\frac{\partial^2 \chi^{(\mathrm{VII})}}{\partial Q^2} + \frac{\partial^2 \chi^{(\mathrm{VII})}}{\partial \theta^2} - \frac{n}{4}\left(1 - \frac{1}{n}\right)^2 \chi^{(\mathrm{VII})} = 0, \tag{92}$$

$$\chi^{(\mathrm{VII})}|_{\theta=0} = (1-\lambda)\exp\left(-n\frac{Q}{2} - \frac{Q}{2}\right), \tag{93}$$

$$\tan\theta \frac{\partial \chi^{(\mathrm{VII})}}{\partial \theta} - \chi^{(\mathrm{VII})} = 0 \qquad \text{on} \quad \theta = \arccos(e^{-nQ}). \tag{94}$$

Matching to region II as $Q \to 0$ leads to the further condition

$$\chi^{(\mathrm{VII})} \sim \left[\frac{2(1-\lambda)}{\pi^{1/2}}\right]\left(\frac{Q^{1/2}}{\theta}\exp\left(-\frac{\theta^2}{4Q}\right)\right)\exp\left(-\frac{nQ}{2}\right) \qquad \text{as} \quad Q \to 0,$$

in view of which we make the WKBJ ansatz

$$\chi^{(\mathrm{VII})} = \left(g_0(Q,\theta) + \frac{1}{n} g_1(Q,\theta) + \cdots \right) \exp\left(-\frac{nQ}{2} \right),$$

leading to the following initial-value problem for g_0 (which is again a parabolic approximation):

$$g_{0,Q} = g_{0,\theta\theta} + \frac{g_0}{2}, \tag{95}$$

$$g_0|_{\theta=0} = (1-\lambda)\exp\left(-\frac{Q}{2}\right), \quad g_{0,\theta}\big|_{\theta=\pi/2} = 0, \tag{96}$$

$$g_0|_{Q=0} = 0, \qquad g_0 \to 0 \quad \text{as} \quad Q \to \infty. \tag{97}$$

We also require the inversion formula, (29) to (31), to give the variables x, y, ψ, these being approximated by

$$\begin{gathered} x \sim -\exp\left(\frac{Q}{2}\right)\left(g_0 \sin\theta + g_{0,\theta}\cos\theta\right), \quad y \sim \lambda - \exp\left(\frac{Q}{2}\right)\left(g_{0,\theta}\sin\theta - g_0\cos\theta\right), \\ \psi \sim \lambda - n^{-1}\exp\left(-nQ + \frac{Q}{2}\right)\left(g_{0,Q} + \frac{g_0}{2}\right). \end{gathered} \tag{98}$$

Solving (95) to (97) for g_0 gives

$$\chi^{(\mathrm{VII})} \sim g_0(Q,\theta)\exp\left(-n\frac{Q}{2}\right),$$

$$\begin{aligned} g_0 = {} & \frac{2(1-\lambda)}{\pi}\exp(-Q/2)\left(2Q\sin\theta + \left(\frac{\pi}{2} - \theta\right)\cos\theta\right) \\ & + \sum_{m=0}^{\infty} A_m \sin((2m+1)\theta)\exp\left(-\left((2m+1)^2 - \frac{1}{2}\right)Q\right), \end{aligned}$$

$$A_0 = -\frac{1-\lambda}{\pi}, \qquad A_m = -\frac{(1-\lambda)}{\pi}\left(\frac{1}{m+1} + \frac{1}{m}\right) \quad \text{for } m \geqslant 1.$$

The finger boundary (corresponding to $\theta \sim \pi/2$) decays exponentially as $x \to -\infty$ to the constant value $y = \lambda$. To leading order, the streamlines are given by the level sets of Q except (in view of $(98)_3$) close to the line $\theta = 0$, on which $g_{0,Q} + g_0/2 = 0$. These streamlines are plotted in Fig. 10.

5. The physical plane

In this section a partial asymptotic solution to the Saffman–Taylor problem for the streamfunction is presented in physical coordinates (10) to (13). In order to tie this together with the solution found in section 4 for the same problem in the Legendre plane we use the same labels for the various asymptotic regions; these are illustrated in Figs 5 and 6, which show the Legendre and physical planes respectively.

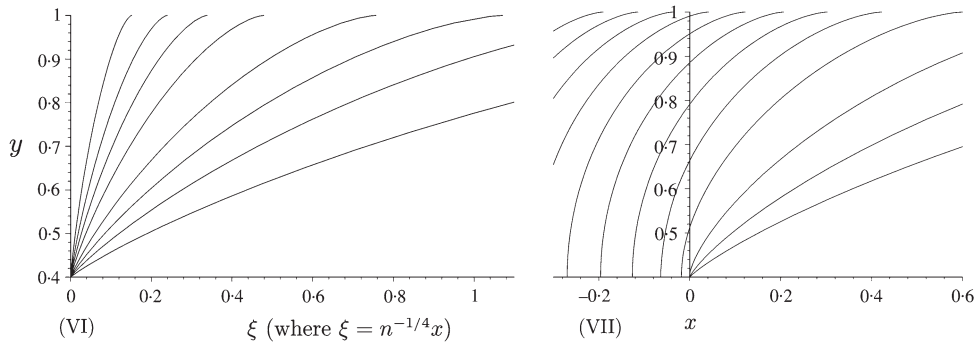

Fig. 10 Approximate streamlines in the physical plane determined from regions VI and VII of the Legendre plane. From the bottom right the streamlines in VII are $\tilde{q} = 0{\cdot}02, 0{\cdot}05, 0{\cdot}1, 0{\cdot}2, 0{\cdot}5, 1, 2, 5$ (where $\tilde{q} \sim -\log(n^{1/2}(\lambda - \psi))/n^{1/2}$), while in (VII) they are $Q = 0{\cdot}05, 0{\cdot}1, 0{\cdot}2, \ldots, 0{\cdot}9, 1{\cdot}0$ (where $Q \sim -\log(\lambda - \psi)/n$). The finger corresponds under these scalings to the semi-infinite strip $x < 0$ (that is, $\xi < 0$), $-0{\cdot}4 < y < 0{\cdot}4$. As $\tilde{q} \to +\infty$ in region VI the solution matches into the solution in region VII as $Q \to 0$

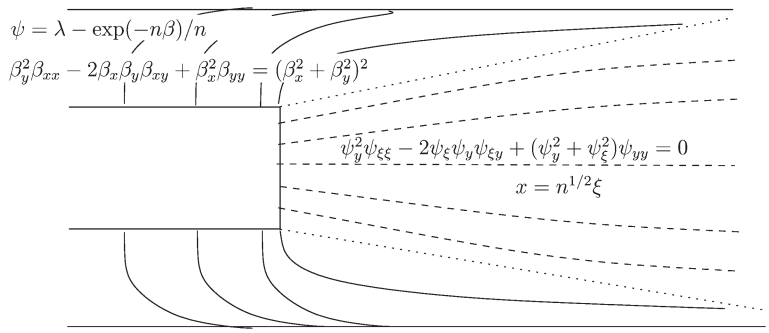

Fig. 11 A schematic of the streamlines in the physical plane, together with the leading-order equations. In the regions where the streamlines correspond to rays they are shown as solid lines. Divisions between regions are shown in dotted lines

5.1 *Remarks on the merits of solving in the Legendre plane versus those of solving in the physical plane*

Note that, whereas the leading-order solutions in regions VI and VII are independent of the solutions in other regions, those in regions II, III, IV, V all depend, via matching conditions, on the leading-order solution in region I (which cannot be solved for directly in the physical plane, that is, without the use of either a Legendre or hodograph transform); the linearizing transformation is thus invaluable in extracting matching conditions on the problems satisfied in regions II, III, IV, V of the physical plane.

5.2 *Slowly varying region in front of the advancing finger* (*region* I)

In light of the scalings derived in section 4.1.2, that is (42), we rewrite (10) to (13) by rescaling x according to

$$x = n^{1/2}\xi$$

and writing the free boundary in the form

$$\xi = \frac{1}{n}\Xi(y;n);$$

since $\Xi = O(1)$, this will allow us to linearize the free-boundary conditions onto $\xi = 0$ (we remark that the scalings $x = O(1)$ and $x = O(n^{-1/2})$ might also be thought pertinent in approaching the free boundary, but these regions turn out to be entirely passive, ψ being given by the inner limit of the $\xi = O(1)$ solution). Thus (10) to (13) give

$$\left(\psi_y^2 + \frac{1}{n^2}\psi_\xi^2\right)\psi_{\xi\xi} - 2\left(1 - \frac{1}{n}\right)\psi_\xi\psi_y\psi_{\xi y} + (\psi_y^2 + \psi_\xi^2)\psi_{yy} = 0, \tag{99}$$

$$\left(-\Xi'(y)\psi_y + \psi_\xi\right)\big|_{\xi=\Xi(y)/n,\,0<y<\lambda} = 0, \qquad \psi|_{\xi=\Xi(y)/n,\,0<y<\lambda} = y, \tag{100}$$

$$\psi|_{y=0} = 0, \qquad \psi|_{y=1} = \lambda, \qquad \psi \to \lambda y \quad \text{as } \xi \to \infty. \tag{101}$$

Expanding ψ and Ξ in powers of $1/n$ in the form

$$\psi = \psi_0^{(\mathrm{I})} + \frac{1}{n}\psi_1^{(\mathrm{I})} + \cdots, \quad \Xi = \Xi_0 + \cdots,$$

and substituting into (99) to (101) leads to an elliptic boundary-value problem for $\psi_0^{(\mathrm{I})}$, namely

$${\psi_0^{(\mathrm{I})}}_y^2\,{\psi_0^{(\mathrm{I})}}_{\xi\xi} - 2{\psi_0^{(\mathrm{I})}}_\xi\,{\psi_0^{(\mathrm{I})}}_y\,{\psi_0^{(\mathrm{I})}}_{\xi y} + \left({\psi_0^{(\mathrm{I})}}_y^2 + {\psi_0^{(\mathrm{I})}}_\xi^2\right){\psi_0^{(\mathrm{I})}}_{yy} = 0, \tag{102}$$

$$\psi_0^{(\mathrm{I})}|_{\xi=0,\,0<y<\lambda} = y, \qquad \psi_0^{(\mathrm{I})}|_{\xi=0,\,\lambda<y<1} = \lambda, \tag{103}$$

$$\psi_0^{(\mathrm{I})}|_{y=0} = 0, \qquad \psi_0^{(\mathrm{I})}|_{y=1} = \lambda, \quad \psi_0^{(\mathrm{I})} \to \lambda y \quad \text{as } \xi \to \infty. \tag{104}$$

Here (102) is the inverse Legendre transform of (32) and the condition $(103)_2$ arises from matching into region VI where $\lambda - \psi$ is exponentially small. Finally $(100)_1$ gives rise to a condition which determines the shape of the free boundary

$$\Xi_0'(y) = \left.\frac{{\psi_0^{(\mathrm{I})}}_\xi}{{\psi_0^{(\mathrm{I})}}_y}\right|_{\xi=0,\,y<\lambda}.$$

Noteworthy features of the solution in this region are (i) that the finger shape, determined here, is to leading order flat running parallel to the y-axis between $y = -\lambda$ and $y = \lambda$, and (ii) that the Aronsson ray approach does not apply in this outer region (slowly varying in x) despite a significant fluid flow. We remark also that (102) has an interesting status as a limit problem of $(1)_1$, notably in that it is a 'slender' limit of an elliptic equation (whose most familiar limit form is parabolic) whereby the

formulation remains elliptic—this may be contrasted with linear elliptic problems whose standard slender approximations are parabolic; we observe that in divergence form it reads (on dropping the suffices) as

$$\frac{\partial}{\partial\xi}\left(\frac{\psi_\xi}{\psi_y}\right)+\frac{\partial}{\partial y}\left(\log\psi_y-\frac{1}{2}\frac{\psi_\xi^2}{\psi_y^2}\right)=0.$$

5.3 *Reformulation in polar coordinates*

At this stage it is useful to introduce polar coordinates about the finger 'corner' (we now choose the origin of x to fix this at $(x, y) = (0, \lambda)$ by setting $B_0 = B_1 = 0$ in (36) and (46))

$$r=\left(x^2+(y-\lambda)^2\right)^{1/2},\quad \phi=\arctan\left(\frac{y-\lambda}{x}\right), \tag{105}$$

in terms of which (10) and (11) can be written as

$$\left(\frac{\psi_\phi^2}{r^2}+\frac{\psi_r^2}{n}\right)\psi_{rr}-2\left(1-\frac{1}{n}\right)\frac{\psi_r\psi_\phi\psi_{r\phi}}{r^2}$$
$$+\frac{1}{r^2}\left(\psi_r^2+\frac{\psi_\phi^2}{nr^2}\right)\psi_{\phi\phi}+\frac{\psi_r^3}{r}+\left(2-\frac{1}{n}\right)\frac{\psi_r\psi_\phi^2}{r^3}=0, \tag{106}$$

$$\psi_r N_r+\frac{\psi_\phi}{r}N_\phi\Big|_{\partial\Omega_f}=0,\quad \psi|_{\partial\Omega_f}=\lambda+r\sin\phi, \tag{107}$$

where the normal to the boundary is $\boldsymbol{N}=N_r\boldsymbol{e}_r+N_\phi\boldsymbol{e}_\phi$.

The physical domains corresponding to all of the regions II, III and IV of the Legendre plane lie close to $(x, y) = (0, \lambda)$. In order to determine the solution in these regions it is convenient to use the formulation (106), (107). In addition, we need to introduce a stretched variable R, to describe the free boundary in terms of R via

$$r=\exp(-n^{1/2}R),\qquad R|_{\partial\Omega}=F(\phi)$$

and to rewrite ψ in the WKBJ form

$$\psi=\lambda-\exp(-n^{1/2}\Upsilon(R,\phi));$$

thus r is exponentially close to zero and ψ to λ. In terms of these new variables (106), (107) give

$$\Upsilon_\phi^2\left(\Upsilon_R+\Upsilon_\phi^2\right)+\frac{1}{n}\left(\Upsilon_R^3+2\Upsilon_R^2\Upsilon_\phi^2-\Upsilon_R\Upsilon_\phi^2\right)+\frac{1}{n^2}\left(\Upsilon_R^4-\Upsilon_R^3\right)$$
$$=\frac{1}{n^{1/2}}\left(\Upsilon_{RR}\Upsilon_\phi^2-2\Upsilon_R\Upsilon_\phi\Upsilon_{R\phi}+\Upsilon_{\phi\phi}\left(\Upsilon_R^2+\Upsilon_\phi^2\right)\right)$$
$$+\frac{2}{n^{3/2}}\Upsilon_R\Upsilon_\phi\Upsilon_{R\phi}+\frac{1}{n^{5/2}}\Upsilon_R^2\Upsilon_{RR}, \tag{108}$$

$$nF'(\phi)\frac{\partial\Upsilon}{\partial\phi}-\frac{\partial\Upsilon}{\partial R}\Big|_{R=F(\phi)}=0,\quad \Upsilon|_{R=F(\phi)}=F(\phi)-\frac{1}{n^{1/2}}\log(-\sin\phi). \tag{109}$$

In addition we must impose the far-field condition

$$\Upsilon \to +\infty \quad \text{as } R \to 0^+ \quad \text{with } \phi > 0, \tag{110}$$

which is equivalent to requiring that $\psi \sim \lambda$ for $r = O(1)$ and $\phi > 0$.

5.4 *Regions* II *and* III

The expansion for Υ in regions II and III proceeds as follows:

$$\Upsilon = \Upsilon_0 + \frac{\log n}{n^{1/2}}\Upsilon_1 + \frac{1}{n^{1/2}}\Upsilon_2 + \cdots,$$

and gives, on substitution into (108),

$$\left(\frac{\partial \Upsilon_0}{\partial \phi}\right)^2 \left(\frac{\partial \Upsilon_0}{\partial R} + \left(\frac{\partial \Upsilon_0}{\partial \phi}\right)^2\right) = 0.$$

This factorization corresponds to two distinct regions, II and III.

5.4.1 *Region* II.

Here the leading-order balance is

$$\frac{\partial \Upsilon_0^{(\mathrm{II})}}{\partial R} + \left(\frac{\partial \Upsilon_0^{(\mathrm{II})}}{\partial \phi}\right)^2 = 0,$$

corresponding to equation (56) in the Legendre plane. Imposing the far-field condition (110) specifies the solution uniquely as

$$\Upsilon_0^{(\mathrm{II})} = \frac{\phi^2}{4R}.$$

In turn this implies that

$$\log(\lambda - \psi^{(\mathrm{II})}) \sim -n\frac{\phi^2}{4\log(1/r)}.$$

5.4.2 *Region* III.

Here the solution satisfies the following leading-order balance and boundary condition (derived from (109)):

$$\frac{\partial \Upsilon_0^{(\mathrm{III})}}{\partial \phi} = 0, \quad \left.\frac{\partial \Upsilon_0^{(\mathrm{III})}}{\partial \phi}\right|_{R=F(\phi)} = 0, \quad \left.\Upsilon_0^{(\mathrm{III})}\right|_{R=F(\phi)} = F(\phi),$$

and consequently has solution

$$\Upsilon_0^{(\mathrm{III})} = R \Longrightarrow \log(\lambda - \psi^{(\mathrm{III})}) \sim \log r.$$

5.5 *Region* IV

In light of the scalings derived from region IV of the Legendre plane (74) we look for a solution in region IV of the physical plane of the form

$$\Upsilon^{(\mathrm{IV})} = \Upsilon^{(\mathrm{IV})}(R, \bar{\phi}), \quad \text{where} \quad \phi = \frac{\pi}{2} + \frac{\bar{\phi}}{n^{1/2}}.$$

Going to leading order gives $\Upsilon^{(\mathrm{IV})}_{0,\bar{\phi}} = 0$ so, in light of (74) we expect $\Upsilon^{(\mathrm{IV})}_0(R) = \pi^2/(16R)$; however, this requires some tricky matching to region II to confirm this.

5.6 *Region* V

In light of the scalings (85) in the Legendre plane, we look for a solution in region V of the physical plane of the form

$$x = n^{-1/2} \log n \exp\left(-\frac{n^{1/2}\pi}{4}\right) X, \qquad y = \lambda - \log n \exp\left(-\frac{n^{1/2}\pi}{4}\right) Y,$$

$$\psi^{(V)} = \lambda - n^{-1} \log n \exp\left(-\frac{n^{1/2}\pi}{4}\right) \hat{\psi},$$

and a free boundary shape described by

$$Y = \frac{1}{n}\Lambda(X).$$

Substituting the above into (10) to (13) gives the following problem for $\hat{\psi}$:

$$\left(\hat{\psi}_Y^2 + \hat{\psi}_X^2\right)\hat{\psi}_{XX} - 2\left(1 - \frac{1}{n}\right)\hat{\psi}_X\hat{\psi}_Y\hat{\psi}_{XY} + \left(\hat{\psi}_X^2 + \frac{1}{n^2}\hat{\psi}_Y^2\right)\hat{\psi}_{YY} = 0, \tag{111}$$

$$-\Lambda'(X)\hat{\psi}_X + \hat{\psi}_Y\Big|_{Y=\Lambda(X)/n} = 0, \quad \hat{\psi}\Big|_{Y=\Lambda(X)/n} = \Lambda(X). \tag{112}$$

The expansion of $\hat{\psi}$ in region V proceeds as follows:

$$\hat{\psi} = \hat{\psi}_0 + \frac{1}{\log n}\hat{\psi}_1 + \cdots,$$

and the equation satisfied by $\hat{\psi}_0$ corresponds to (83) in the Legendre plane, (111) being equivalent to (102) but with the roles of x and y interchanged, and the free-boundary conditions similarly linearize on to $Y = 0$, where

$$\hat{\psi}_{0,Y} = \hat{\psi}_{0,X}^2.$$

5.7 *The problem about the top edge of the finger* (*region* VII)

In light of the scalings for the physical variables (98) derived in section 4.7 we look for a solution in the physical plane, along the top edge of the finger (see Fig. 6), of the form

$$\psi = \lambda - \frac{1}{n}\exp(-n\beta(x, y)). \tag{113}$$

Substituting this ansatz into (6) gives

$$\left(\beta_y^2+\frac{1}{n}\beta_x^2\right)\beta_{xx}-2\left(1-\frac{1}{n}\right)\beta_x\beta_y\beta_{xy}+\left(\beta_x^2+\frac{1}{n}\beta_y^2\right)\beta_{yy}=\left(\beta_x^2+\beta_y^2\right)^2. \tag{114}$$

On the upper boundary $(13)_1$ gives

$$\beta\to+\infty \quad \text{as } y\nearrow 1. \tag{115}$$

The condition $\psi|_{\partial\Omega}=y$ implies that the finger shape is given by

$$y=\lambda-\frac{1}{n}\exp(-n\beta),$$

while $(11)_1$ gives

$$\left(\beta_y-|\nabla\beta|^2e^{-n\beta}\right)\Big|_{y=\lambda-\exp(-n\beta)/n}=0.$$

Linearizing on to $y=\lambda$ gives the approximate boundary condition

$$\beta_y|_{y=\lambda}=0. \tag{116}$$

To close the problem for β we match to the main flow (corresponding to region I of the Legendre plane); this gives

$$\beta\sim O\left(\frac{1}{n}\right) \quad \text{as } x\to+\infty, \quad \beta\sim O\left(\frac{1}{n}\right) \quad \text{as } y\to\lambda \quad \text{with } x>0. \tag{117}$$

Whilst it is not possible to solve the full problem comprised of (114) to (117), without recourse to Legendre or Hodograph transforms, we can solve this problem in the limit $x\to-\infty$. This subproblem is invariant under translations of x and β, which suggests looking for a solution of the form

$$\beta_0=-kx+G(y).$$

This gives rise to the following problem for G and k:

$$\left(k^2+\frac{1}{n}\left(\frac{dG}{dy}\right)^2\right)\frac{d^2G}{dy^2}=\left(k^2+\left(\frac{dG}{dy}\right)^2\right)^2, \tag{118}$$

$$\left.\frac{dG}{dy}\right|_{y=\lambda}=0, \tag{119}$$

$$G\to\infty \quad \text{as} \quad y\to 1, \tag{120}$$

which, on introduction of the variable $z=dG/dy$, can be analysed by use of a phase plane. The naive asymptotic expansion $G=G_0+O(1/n)$ gives rise to a leading-order equation for G_0 which is incompatible with the boundary condition (120). In order to overcome this difficulty we introduce an outer region in which $1-y=O(1)$, and on which the boundary condition

$$dG/dy\to\infty \quad \text{as} \quad y\to 1 \tag{121}$$

is imposed, and match to an inner region where $1-y=O(n^{-3/2})$.

5.7.1 *Outer region* VII. Expanding z and k as follows:

$$G^o = G_0^o + O\left(\frac{1}{n}\right), \quad z^o = z_0^o + O\left(\frac{1}{n}\right), \quad k = k_0 + O\left(\frac{1}{n}\right),$$

and substituting into (118), (119) and (121) gives the leading-order outer problem

$$\frac{dz_0^o}{dy} = \frac{1}{k_0^2}(k_0^2 + z_0^{o2})^2, \quad z_0^o|_{y=\lambda} = 0, \quad z_0^o \to +\infty \quad \text{as} \quad y \to 1.$$

This has solution

$$\frac{z_0^o}{k_0^2 + z_0^{o2}} + \frac{1}{k_0}\arctan\left(\frac{z_0^o}{k_0}\right) = 2(y - \lambda), \qquad k_0 = \frac{\pi}{4(1-\lambda)}.$$

Although z_0^o is infinite on $y = 1$, having the behaviour

$$z_0^o \sim \left(\frac{\pi^2}{48(1-\lambda)}\right)^{1/3}(1-y)^{-1/3},$$

G_0^o is not and so does not satisfy (120). This requires the introduction of an inner region about $y = 1$. The streamlines given by this outer solution (corresponding to a contour plot of $\beta_0^o = -kx + G_0^o(y)$) are shown in Fig. 12.

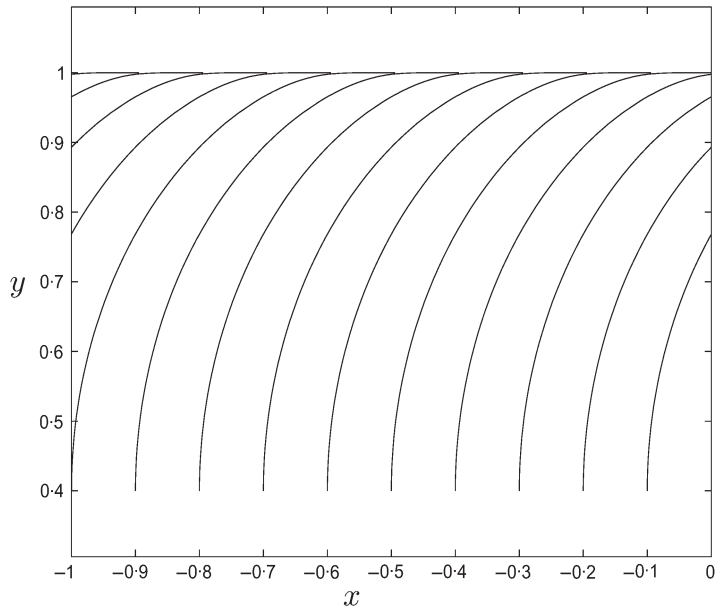

Fig. 12 The streamlines in region VII calculated from the leading-order outer solution for β, namely $\beta \sim -kx + G_0^o(y)$, in the case $\lambda = 0{\cdot}4$

5.7.2 *Inner region* VII. Introducing inner variables

$$y = 1 - n^{-3/2}\eta, \quad z^i = n^{1/2} z_0^i + n^{-1/2} z_1^i + \cdots,$$

substituting into (118) and (120) and matching to the outer region gives the following leading-order problem for z_0^i:

$$\frac{dz_0^i}{d\eta} = -\frac{z_0^i}{k_0^2 + {z_0^i}^2},$$

$$z_0^i \to +\infty \quad \text{as } \eta \to 0, \quad z_0^i \sim \left(\frac{\pi^2}{48(1-\lambda)}\right)^{1/3} \eta^{-1/3} \quad \text{as } \eta \to +\infty,$$

with solution

$$\frac{k_0^2}{3{z_0^i}^3} + \frac{1}{z_0^i} = \eta.$$

Note that this solution satisfies the required far-field behaviour and that

$$z_0^i \sim \frac{1}{\eta} \quad \text{as} \quad \eta \to 0 \Longrightarrow G^i \sim \text{const.} - \frac{1}{n}\log\eta \quad \text{as } \eta \to 0,$$

which implies that it also satisfies (120).

5.8 *The flow between the finger corner and the top boundary of the cell* (*region* VI)

Here we look for a solution in the physical plane (for $\lambda < y < 1$, $x > 0$) corresponding to region VI of the Legendre plane (see Fig. 6). In light of the scalings for the physical variables (90) derived in section 4.7 we adopt the following ansatz:

$$\psi = \lambda - \frac{1}{n^{1/2}} \exp(-n^{1/2}\alpha(\xi, y)), \quad x = n^{1/4}\xi.$$

Substituting into (10) and $(13)_1$, matching to the central region of the flow and to that along the top edge gives

$$\left(\alpha_y^2 + \frac{1}{n^{3/2}}\alpha_\xi^2\right)\alpha_{\xi\xi} - 2\left(1 - \frac{1}{n}\right)\alpha_\xi\alpha_y\alpha_{\xi y} + \left(\alpha_\xi^2 + \frac{1}{n^{1/2}}\alpha_y^2\right)\alpha_{yy}$$

$$= \alpha_y^4 + 2\frac{1}{n^{1/2}}\alpha_\xi^2\alpha_y^2 + \frac{1}{n}\alpha_\xi^4, \tag{122}$$

$$\alpha \to +\infty \quad \text{as } y \to 1, \qquad \alpha \to 0 \quad \text{as } y \to \lambda, \tag{123}$$

$$\alpha \to 0 \quad \text{as } \xi \to \infty, \qquad \alpha \to +\infty \quad \text{as } \xi \to 0. \tag{124}$$

In the discussion in section 4.6 (which treats region VI in the Legendre plane) we noted that this region subdivides into two regions in the physical plane. We now go on to consider these.

Performing a hodograph transformation on the leading-order problem from (122) by introducing an artificial time variable t and setting $t = \alpha_0$, $y = \zeta(\xi, t)$, yields the singular parabolic equation

$$\frac{\partial\zeta}{\partial t} = -\left(\frac{\partial^2\zeta}{\partial\xi^2}\right)^{-1} \tag{125}$$

which is, as is well known, linearized by a Legendre transformation; the required solution to (125) is of the self-similar form $\zeta = \zeta(\xi t^{1/2})$.

5.8.1 *Outer region* VI. To leading order this problem is invariant under $\xi \to \xi/k$, $\alpha \to k^2\alpha$ which suggests looking for a solution of the form

$$\alpha^o = \frac{H(y)}{\xi^2} + n^{-1/2}\alpha_1^o + \cdots .$$

Substituting into (122), (123) and taking the leading-order term gives

$$4H^2\frac{d^2H}{dy^2} - 2H\left(\frac{dH}{dy}\right)^2 - \left(\frac{dH}{dy}\right)^4 = 0, \tag{126}$$

$$H(\lambda) = 0, \qquad H \to \infty \quad \text{as } y \to 1, \tag{127}$$

which corresponds to equation (88) in the Legendre plane. It is possible to integrate (126) exactly, however, it is not possible to satisfy the boundary condition $(127)_2$ and, in light of the comments made at the end of section 4.6, we look for a solution which satisfies

$$\frac{dH}{dy} \to \infty \quad \text{as } y \to 1.$$

This gives, in conjunction with (126) and $(127)_1$

$$y - 1 = (2H_0)^{1/2}\left(\left(\log\left(\frac{H_0}{H}\right)\right)^{1/2}\left(\frac{H}{H_0}\right)^{1/2} - \left(\frac{\pi}{2}\right)^{1/2}\operatorname{erf}\left(\frac{1}{\sqrt{2}}\left(\log\left(\frac{H_0}{H}\right)\right)^{1/2}\right)\right),$$

where

$$H_0 = \frac{1}{\pi}(1-\lambda)^2.$$

The behaviour of H as y approaches 1 is thus

$$H \sim H_0\left(1 - \left(\frac{3(1-y)}{(2H_0)^{1/2}}\right)^{2/3}\right) \qquad \text{as } y \nearrow 1.$$

A contour plot of $\alpha_0^o = H(y)/\xi^2$ (showing typical streamlines) is given in Fig. 13.

5.8.2 *Inner region* VI. In order to satisfy the boundary condition $(123)_1$ we introduce an inner region by making the following rescaling and ansatz:

$$y = 1 + n^{-3/4}Y, \qquad \alpha^i = f(\xi) + \frac{\hat{\alpha}(\xi, Y)}{n^{1/2}},$$

to obtain

$$\left(\hat{\alpha}_Y^2 + \frac{1}{n^2}\left(f' + \frac{\hat{\alpha}_\xi}{n^{1/2}}\right)^2\right)\left(f'' + \frac{\hat{\alpha}_{\xi\xi}}{n^{1/2}}\right) - 2\left(1 - \frac{1}{n}\right)\left(f' + \frac{\hat{\alpha}_\xi}{n^{1/2}}\right)\hat{\alpha}_Y\hat{\alpha}_{\xi Y}$$

$$+n^{1/2}\left(\hat{\alpha}_Y^2 + \left(f' + \frac{\hat{\alpha}_\xi}{n^{1/2}}\right)^2\right)\hat{\alpha}_{YY} = n^{1/2}\left(\hat{\alpha}_Y^2 + \frac{1}{n}\left(f' + \frac{\hat{\alpha}_\xi}{n^{1/2}}\right)^2\right)^2.$$

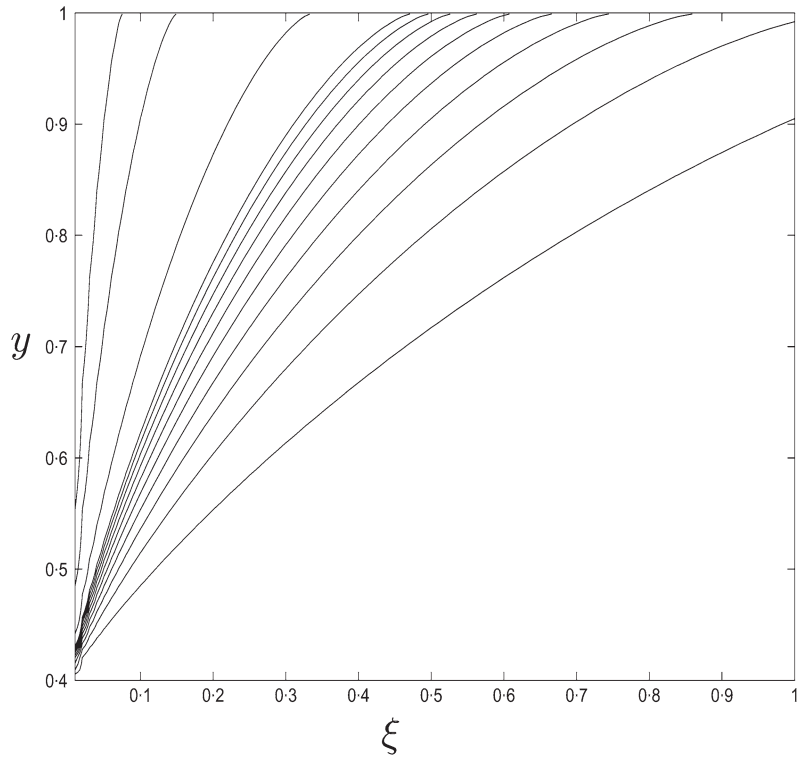

Fig. 13 The streamlines calculated from the leading-order outer solution α^o in region V1, namely $H(y)/\xi^2$, in the case $\lambda = 0{\cdot}4$. Here the streamlines are plotted at values of $\alpha^o = 0{\cdot}05, 0{\cdot}1, \ldots, 0{\cdot}5$, 1, 5 and 20

Making the assumption that $\hat{\alpha} \geqslant O(f)$ (which is justified *a posteriori*) gives the leading-order balance

$$\left(\hat{\alpha}_Y^2 + f'^2(\xi)\right)\hat{\alpha}_{YY} \sim \hat{\alpha}_Y^4. \tag{128}$$

This is a first-order autonomous ODE for $\hat{\alpha}_Y$ (in which ξ appears only as a parameter). Matching to the outer region (at leading order) determines f as

$$f(\xi) = \frac{H_0}{\xi^2}.$$

Proceeding with the matching to next order and applying the condition $(123)_1$ gives boundary data on (128)

$$\hat{\alpha} \to +\infty \quad \text{as } Y \nearrow 0, \qquad \hat{\alpha} \sim -\frac{1}{\xi^2}\left(-\frac{3H_0 Y}{\sqrt{2}}\right)^{2/3} \quad \text{as } Y \to -\infty. \tag{129}$$

Integrating (128) once gives

$$\frac{4H_0^2}{3\xi^6}\left(\frac{\partial\hat{\alpha}}{\partial Y}\right)^{-3} + \left(\frac{\partial\hat{\alpha}}{\partial Y}\right)^{-1} = -Y.$$

The solution to the above exhibits the behaviour $(129)_2$ as $Y \to -\infty$ and, as $Y \to 0$, has the following behaviour:

$$\alpha_1^i \sim \log(-Y) \qquad \text{as } Y \nearrow 0,$$

thus satisfying the boundary condition $(129)_1$.

6. Discussion

In this work we have used the Legendre transform to investigate the structure of the symmetric Saffman–Taylor finger for a power-law fluid in the limit of extreme shear-thinning, as the exponent n approaches $+\infty$, and with zero surface tension. To leading order the finger is a semi-infinite strip (see Fig. 6) with arbitrary width 2λ, its leading edge being described by the equation

$$x = \frac{1}{n^{1/2}}\Xi(y),$$

where $\Xi(\cdot)$ is an $O(1)$ function. Directly in front of the leading edge of the finger there is a region of plug flow (labelled region I) which slowly adjusts itself to the width of the channel over an $O(n^{1/2})$ (dimensionless) distance, in the x-direction. This is separated from regions in which the flow is exponentially small (unyielded in the limit $n \to +\infty$) by shear layers (shadow boundaries in the Legendre plane). The asymptotic structure around the 'corners' of the finger is rather complicated, consisting of four further regions.

A noteworthy feature of analysis is that it is far easier to conduct in the Legendre plane than in the physical plane. This is for two reasons: first the solutions in a number of the asymptotic regions depend (either directly or indirectly) via matching conditions on the solution found in region I and the latter can only be found analytically via a Legendre transform and, secondly, several of the regions in the physical plane are described in terms of logarithmic radial coordinates which makes application of the free boundary conditions and matching to other regions problematic.

In contrast to the extreme shear-thinning power-law injection problem none of the asymptotic regions corresponds to the 'naive' limit problem (as $n \to +\infty$)

$$\nabla \cdot \left(\frac{\nabla \psi}{|\nabla \psi|} \right) = 0 \qquad \text{(or equivalently} \quad |\nabla p| = 1) \,.$$

Consequently the simple arguments used by Aronsson (**11**, **14**, **17** to **19**) to explain the features of the injection problem (and formalized in terms of rigorous asymptotics) do not carry over to the Saffman–Taylor problem.

We have, in the treatment of this problem, tacitly assumed that the finger width λ is $O(1)$ (our analysis also covers the case where the finger is algebraically small in inverse powers of n). Extrapolating from the results presented by Ben Amar and Corvera Poiré (**10**) (for a nearly Newtonian fluid) we might expect that the selected finger width λ, in the limit of small surface tension and large shear-thinning exponent n to be small. This motivates us, in the Appendix, to briefly consider the limit problem for a narrow finger (in the limit $\lambda \to 0$ with $\lambda = o(\exp(-kn))$, where k is a positive $O(1)$ constant).

References

1. P. G. Saffman and G. I. Taylor, The penetration of a fluid into a Hele-Shaw cell containing a more viscous fluid, *Proc. R. Soc.* A **245** (1958) 312.

2. J. W. McLean and P. G. Saffman, The effect of surface tension on the shape of fingers in a Hele-Shaw cell, *J. Fluid Mech.* **102** (1981) 455.

3. R. Combescot, T. Dombre, V. Hakim, Y. Pomeau and A. Pumir, Shape selection of Saffman Taylor fingers, *Phys. Rev. Lett.* **56** (1986) 2036.

4. B. I. Shraiman, Velocity selection in the Saffman Taylor problem, *ibid.* **56** (1986) 2028–2031.

5. X. Xie and S. Tanveer, Rigorous results in steady finger selection in viscous fingering, *Arch. Rat. Mech. Anal.* **166** (2003) 219–286.

6. J. R King and S. J. Chapman, The selection of Saffman–Taylor fingers by kinetic undercooling, *J. Eng. Math.* **46** (2003) 1–32.

7. S. Tanveer, Surprises in viscous fingering, *J. Fluid Mech.* **409** (2000) 273–308.

8. D. A. Kessler and H. Levine, Microscopic selection of fluid fingering patterns, *Phys. Rev. Lett.* **86** (2001) 4532–4535.

9. M. Ben Amar and E. Corvera Poiré, Finger behaviour of shear thinning fluid in a Hele-Shaw cell, *ibid.* **81** (1998) 2048–2051.

10. M. Ben Amar and E. Corvera Poiré, Pushing a non-Newtonian fluid in a Hele-Shaw cell: from fingers to needles, *Phys. Fluids* **11** (1999) 1757–1767.

11. G. Aronsson and U. Janfalk, On Hele-Shaw flows of power law fluids, *Europ. J. Appl. Math.* **3** (1992) 343–366.

12. J. R. King, Development of singularities in some moving boundary value problems, *ibid* **6** (1995) 491–507.

13. A. N. Alexandrou and V. Entov, On the steady-state advancement of fingers and bubbles in a Hele-Shaw cell filled by a non-Newtonian fluid, *ibid.* **8** (1997) 73–87.

14. G. Aronsson, On p-harmonic functions, convex duality and an asymptotic formula for injection moulding, *ibid.* **8** (1996) 417–437.

15. J. R. King, J.R. Ockendon and H. Ockendon, The Laplace–Young equation near a corner, *Q. Jl Mech. Appl. Math.* **52** (1999) 73–97.

16. F. Piscotti, A. Boldizar, M. Rigdahl and G. Aronsson, Evaluation of a model describing the advancing flow front in injection moulding, *Intern. Polymer Proc.* **17** (2002) 133–145.

17. G. Aronsson, Five geometric principles of injection moulding, *ibid.* **18** (2003) 91–94.

18. G. Aronsson and L.C. Evans, An asymptotic model for compression molding, *Indiana Univ. Math. J.* **51** (2002) 1–36.

19. A. Bergwall, A geometric evolution problem, *Quart. Appl. Math.* **50** (2002) 37–73.

20. M. E. Brewster, S. J. Chapman, A. D. Fitt and C. P. Please, Asymptotics of slow flow of very small exponent shear thinning fluids in a wedge, *Europ. J. Appl. Math.* **6** (1995) 559-571.

21. S. J. Chapman, A. D. Fitt and C. P. Please, Extrusion of power law shear thinning fluids with small exponent, *Int. J. Non-Linear Mech.* **32** (1997) 187–199.

22. J. W. Barrett and L. Prighozhin, Beans critical state model as the $p \to \infty$ limit of a p-Laplacian equation, *Nonlinear Anal.* **42** (2000) 977–993.

23. A. Lindner, D. Bonn and J. Meunier, Viscous fingering in a shear thinning fluid, *Phys. Fluids* **12** (2000) 256–261.

24. A. Lindner, D. Bonn, E. Corvera Poire, M. Ben Amar and J. Meunier, Viscous fingering in non-Newtonian fluids, *J. Fluid Mech.* **469** (2002) 237–256.

25. C. Atkinson and C. R. Champion, Some boundary-value problems for the equation $\nabla \cdot (|\nabla\phi|^N \nabla\phi) = 0$, *Q. Jl Mech. Appl. Math.* **37** (1984) 401–419.

26. J.R. King, Two generalisations of the thin film equations, *Math. Comp. Mod.* **34** (2001) 737–756.

APPENDIX

The Ivantsov problem for power-law fluids

The analysis we pursue here applies for more general constitutive assumptions than those above (see (**26**) for a derivation of how $\Omega(|\nabla\psi|)$ below is determined by the constitutive properties of the fluid). We accordingly consider

$$\nabla\cdot(\Omega(|\nabla\psi|)\nabla\psi)=0$$

for rather general $\Omega(\cdot)$, subject to the boundary conditions (11) to (13). Transforming to the Legendre plane yields

$$\rho\Omega(\rho)(\Psi_{aa}+\Psi_{bb})+\Omega'(\rho)(a^2\Psi_{bb}-2ab\Psi_{ab}+b^2\Psi_{aa})=0$$

subject to (18), (19) and hence to

$$\Psi_{\rho\rho}+\frac{1}{\rho}\left(1+\frac{\rho\Omega'(\rho)}{\Omega(\rho)}\right)\left(\Psi_\rho+\frac{1}{\rho}\Psi_{\theta\theta}\right)=0 \tag{A1}$$

subject to (21) to (23), an important feature of (A1) being that Ψ is separable in ρ and θ.

Next we formally set $\lambda=0$ in the boundary conditions to give (21) together with

$$\Psi=0\quad\text{for}\quad 0<\rho<1\quad\text{on}\quad\theta=0 \tag{A2}$$

and observe that both (21) and (A2) can automatically be satisfied by adopting the ansatz

$$\Psi=F(\rho)\sin\theta. \tag{A3}$$

It follows from (A1) that $F(\rho)$ is given by the linear ordinary differential equation

$$\frac{d^2F}{d\rho^2}+\frac{1}{\rho}\left(1+\frac{\rho\Omega'(\rho)}{\Omega(\rho)}\right)\left(\frac{dF}{d\rho}-\frac{1}{\rho}F\right)=0; \tag{A4}$$

it is worth emphasizing that this reduction is somewhat remarkable. One solution of (A4) is given by $F=\mathcal{M}\rho$, corresponding to translations of x and accordingly being (as already noted) irrelevant. The second solution can be obtained by reduction of order in the form

$$F=\mathcal{N}\rho\int_\rho^\infty\frac{1}{\rho'^3\Omega(\rho')}d\rho'; \tag{A5}$$

the mechanism which specifies its amplitude $\mathcal{N}$, via its singularity, is described below. The free boundary $\rho=\cos\theta$ is then given in physical coordinates (parametrically in terms of $\rho=\cos\theta$) from the more general expressions

$$x=-\frac{1}{\rho}F-\frac{1}{\rho}(\rho F'-F)\sin^2\theta,$$
$$y=\frac{1}{\rho}(\rho F'-F)\sin\theta\cos\theta,$$

wherein it follows from (A5) that

$$\rho F'-F=-\frac{\mathcal{N}}{\rho\Omega(\rho)};$$

we remark that

$$\psi=\frac{\rho y}{\cos\theta}$$

holds everywhere.

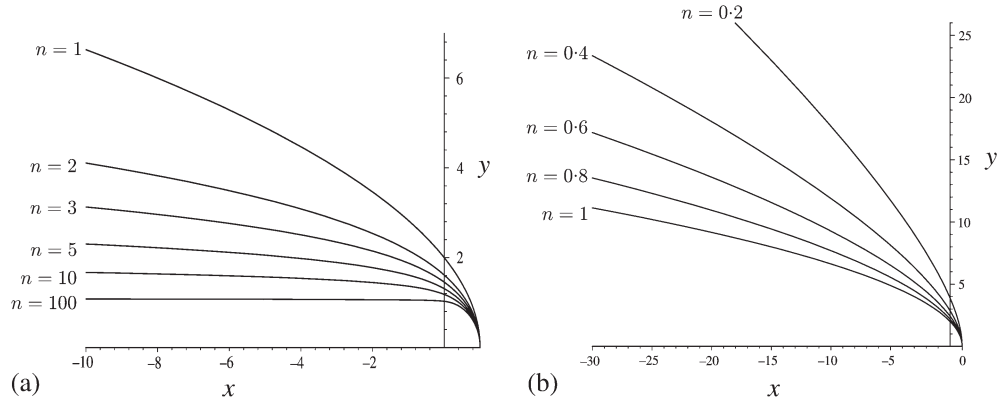

Fig. A The Ivantsov finger with $C = 1$ and for (a) shear thinning fluids $n = 100, 10, 5, 3, 2, 1$ and (b) for shear thickening ones, $n = 0{\cdot}2, 0{\cdot}4, 0{\cdot}6, 0{\cdot}8, 1$

.

In the case of a power-law fluid we have $\Omega(\rho) = \rho^{-(n-1)/n}$ and (A5) becomes

$$F = -C\rho^{-1/n},$$

where $C = -n\mathcal{N}/(n+1)$. It then follows that

$$\begin{aligned} \frac{x}{C} &= \rho^{-(n+1)/n}\left(1 - \frac{n+1}{n}\sin^2\theta\right), \\ \frac{y}{C} &= \frac{n+1}{n}\rho^{-(n+1)/n}\sin\theta\cos\theta, \end{aligned} \tag{A6}$$

and the free boundary $\rho = \cos\theta$ is shown for various values of n in Fig. A. In particular in the Newtonian case $n = 1$ we have

$$\left(\frac{y}{2C}\right)^2 - 1 = \frac{x}{C},$$

giving the usual Ivantsov parabola. The large-x behaviour of the finger shape given by (A6) is

$$y \sim C\left(\frac{n+1}{n}\right)\left(\frac{n(-x)}{C}\right)^{1/(n+1)} \qquad \text{as} \quad x \to -\infty.$$

This is to be compared with the approach of (**10**), which records power-law behaviour

$$y \sim \text{ const. } (-x)^{1/(n+1)}$$

over a suitable intermediate regime for slender (needle) Saffman–Taylor fingers.

The above expressions give an exact solution for our class of non-Newtonian Hele-Shaw problem. To describe its relevance to the Saffman–Taylor problem, we now record that it represents, in the limit $\lambda \to 0$, the outer solution in the Legendre plane and the inner solution at the tip of the finger in the physical plane. The outer solution in the physical plane replaces the free-boundary conditions by $\psi_y = 0$ on $y = 0$, $x < 0$ (say, given the invariance of the formulation under translations in x). The associated inner problem in the Legendre plane has scalings

$$a = \lambda\hat{a}, \quad b = \lambda\hat{b}, \quad \Psi = \lambda\hat{\Psi},$$

producing at leading order a quarter-plane problem in $\hat{a} < 0$, $\hat{b} > 0$, with

$$\begin{aligned} &\text{on} \quad \hat{b} = 0 \quad \hat{\Psi}_{\hat{b}} = 0 \qquad \text{for} \quad \hat{a} < 0, \\ &\text{on} \quad \hat{a} = 0 \begin{cases} \hat{\Psi} = \hat{b} - 1 & \text{for} \quad 0 < \hat{b} < 1, \\ \hat{\Psi} = 0 & \text{for} \quad \hat{b} > 1, \end{cases} \end{aligned}$$

hence in terms of polar coordinates the boundary conditions read

$$\begin{aligned} &\text{on} \quad \hat{\rho} = 0 \quad \hat{\Psi} = -1 \qquad \text{for} \quad 0 < \theta < \tfrac{1}{2}\pi, \\ &\text{on} \quad \theta = 0 \begin{cases} \hat{\Psi} = \hat{\rho} - 1 & \text{for} \quad 0 < \hat{\rho} < 1, \\ \hat{\Psi} = 0 & \text{for} \quad \hat{\rho} > 1, \end{cases} \\ &\text{on} \quad \theta = \tfrac{1}{2}\pi \qquad\qquad \hat{\Psi}_\theta = 0, \end{aligned}$$

and this boundary-value problem has been solved in a different context in (**25**). The inner boundary-value problem determines $\hat{\Psi}$ uniquely, in contrast to the outer one in which Ψ is determined only up to an arbitrary multiplicative constant $\mathcal{N}$; once the inner solution is known, $\mathcal{N}$ is easily determined by matching its far field $\hat{\rho} \to +\infty$ with (A5) with $\rho \to 0$. Thus we have from (**25**) that

$$\hat{\Psi} \sim -\frac{4n^2}{\pi(n+1)^2}\hat{\rho}^{-1/n}\sin\theta \qquad \text{as} \quad \hat{\rho} \to +\infty,$$

so that

$$\mathcal{N} = -\lambda^{1+1/n}\frac{4n}{\pi(n+1)}.$$